# Advanced Topics in Fluid Dynamics of Climate

John R. Taylor (J.R.Taylor@damtp.cam.ac.uk)

# 1 A Simple model for the Hadley Cell

See Gill §9.16

At the start of the Fundamentals course, we talked about the primary wind patterns in the atmosphere. These patterns are shown again in Figure 1. At this point, we know enough about rotating flows to understand why some of these patterns are formed. Two important features of the near-surface winds are the *cyclonic* westerlies at mid-latitudes, and the *anticyclonic* trade winds at low latitudes.

Recall from the Fundamentals course that the mid-latitude westerlies can be explained by combining several two basic concepts. Start by assuming that the velocity is in geostrophic balance:

$$2\boldsymbol{\Omega} \times \mathbf{u}_g = \frac{1}{\rho}\nabla p, \tag{1.1}$$

or in vector notation

$$f\mathbf{u}_g = \hat{\mathbf{z}} \times \frac{\nabla p}{\rho}, \tag{1.2}$$

where we have retained only the vertical component of the rotation vector, i.e. $\Omega = (0, 0, f/2)$. If the pressure is in hydrostatic balance, then

$$\frac{\partial p}{\partial z} = -\rho\frac{g}{\rho_0}. \tag{1.3}$$

If we further assume that the density is a linear function of temperature:

$$\rho = \rho_0(1 - \alpha(T - T_0)), \tag{1.4}$$

where $\alpha$ is the thermal expansion coefficient and $T_0$ and $\rho_0$ are the reference temperature and density. Combining these three equations gives the *thermal wind* relation

$$\frac{\partial \mathbf{u}_g}{\partial z} = \frac{\alpha g}{f}\hat{\mathbf{z}} \times \nabla T. \tag{1.5}$$

The midlatitudes have a strong equatorward temperature gradient, which produces a thermal wind flowing from west to east (Note that $f$ is negative in the Southern hemisphere).

The trade winds are slightly more subtle, but can be explained using a simple model. The trade winds arise in direct response to heating of the atmosphere near the equator. Consider rotating flow driven by an interior buoyancy source, $\mathcal{F}_B$. For simplicity, we will consider the linearized equations in hydrostatic balance:

$$u_t - fv = -\frac{1}{\rho_0}p_x - ru, \tag{1.6}$$

$$v_t + fu = -\frac{1}{\rho_0}p_y - rv, \tag{1.7}$$

$$p_z = \rho_0 b, \tag{1.8}$$

$$u_x + v_y + w_z = 0, \tag{1.9}$$

$$b_t = \mathcal{F}_B - \alpha b. \tag{1.10}$$

The last terms in the momentum equations are called 'Rayleigh friction', and act like an artificial frictional drag. Similarly, $\alpha$ is a 'Newtonian cooling' term which reduces the buoyancy and can balance the buoyancy source $\mathcal{F}_B$ in an integrated sense. Consider the flow on an $f$-plane where $x$ points to the west, $y$ points to

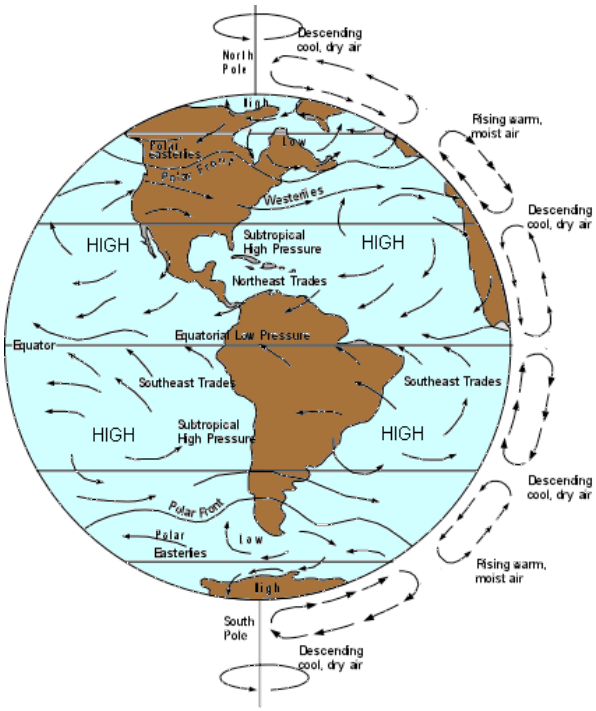


Figure 1: Atmospheric wind patterns (http://msnucleus.org/)

the north, and $z$ is aligned with the local gravity. Then, let's look for steady, zonally symmetric solutions $(\partial_t, \partial_x = 0)$. The continuity equation simplifies to

$$v_y + w_z = 0, \tag{1.11}$$

from which we see that we can define a *meridional overturning stream function*, $\psi$, so that

$$v = -\psi_z, \quad w = \psi_y. \tag{1.12}$$

The zonal momentum equation also simplifies to

$$fv = ru, \tag{1.13}$$

and an equatorward velocity in the northern hemisphere ($v < 0$) is balanced by a westward flow ($u < 0$). Eqns. (1.10) can be combined into a single equation for the streamfunction

$$(f^2 + r^2)\psi_{zz} = \frac{r}{\alpha}\frac{\partial \mathcal{F}_B}{\partial y}. \tag{1.14}$$

To solve for $\psi$, we need to specify the buoyancy forcing. A simple example is

$$\mathcal{F}_B = B_0(1 - z)\cos y, \tag{1.15}$$

which is maximum at the equator ($y = 0$) and the ground ($z = 0$) and goes to zero at the top of the atmosphere ($z = 1$). Although this is clearly a drastic simplification of the actual radiative forcing in the atmosphere, it does capture the gross features (see Figures 2 and 3).

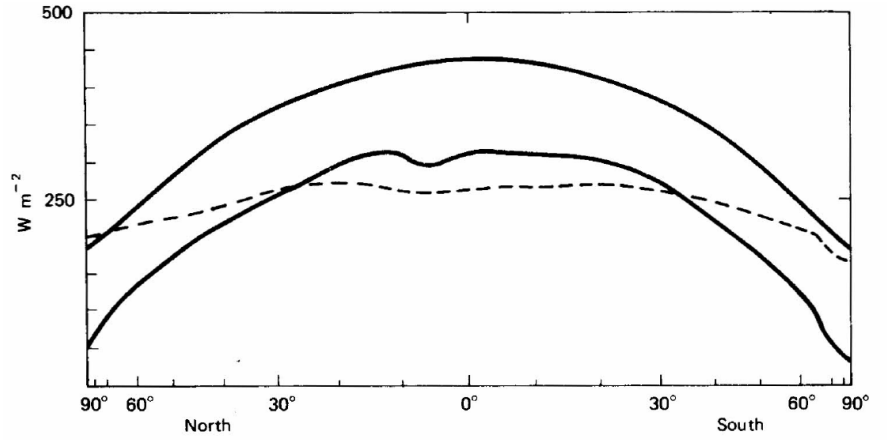


**Fig. 1.1.** The radiation balance of the earth. The upper solid curve shows the average flux of solar energy reaching the outer atmosphere. The lower solid curve shows the average amount of solar energy absorbed; the dashed line shows the average amount of outgoing radiation. The lower curves are average values from satellite measurements between June 1974 and February 1978, and are taken from Volume 2 of Winston *et al.* (1979). Values are in watts per square meter. The horizontal scale is such that the spacing between latitudes is proportional to the area of the earth's surface between them, i.e., is linear in the sine of the latitude.

Figure 2: Global heat balance, from Gill 1982 and revisited from FFMC notes

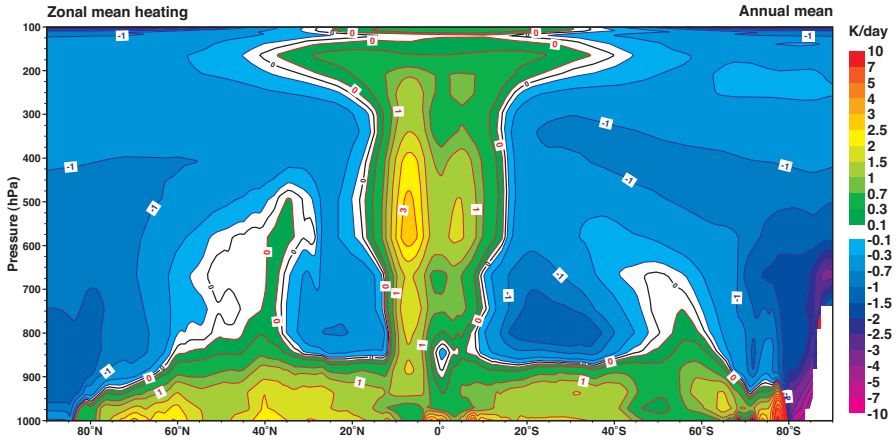


Figure 3: Zonal mean heating, ECMWF, revisited from FFMC notes

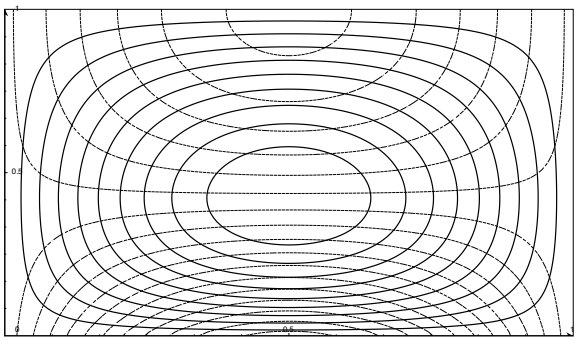

Figure 4: Meridional streamfunction (solid) and zonal flow (dashed)

The streamfuction associated with this forcing is

$$\psi = \frac{-r}{\alpha(f^2+r^2)}\sin y(\frac{z^2}{2} - \frac{z^3}{6} - \frac{z}{3}) \tag{1.16}$$

where we have used $\psi_y = 0$ at $z = 0, 1$ as the boundary conditions. Figure (4) shows the streamfunction, which is an idealized version of the Hadley cell. The flow is equatorward near the ground, and poleward at high latitude. We can find the corresponding zonal flow using Eq. (1.13)

$$u = \frac{f}{r}v = -\frac{f}{r}\psi_z = \frac{f}{\alpha(f^2+r^2)}\sin y(\frac{z}{2} - \frac{z^2}{6} - \frac{1}{3}). \tag{1.17}$$

The zonal flow is shown with dashed lines in Figure (4). Near the ground the flow is to the west ($u < 0$), in the same direction as the trade winds. Note that we haven't imposed a no-slip boundary at the ground. In reality the fact that $u = 0$ at $z = 0$ leads to an Ekman boundary layer, a feature that we will examine in detail later in the course.

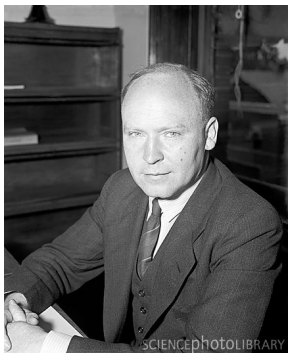

Figure 5: Carl-Gustav Rossby (left) and Hans Ertel (right)

# 2 Potential vorticity

When discussing the conservation of angular momentum in the rotating shallow water equations in FFMC, the potential vorticity (or PV) was briefly defined. PV is a *scalar* quantity which satisfies important conservation equations that strongly constrain the large scale dynamics of the ocean and atmosphere. It is difficult to overstate the importance of concept of PV to the field of geophysical fluid dynamics.

The definition of PV changes slightly depending on the set of governing equations that we consider, but the physical interpretation remains much the same. To see this, let's go back and revisit potential vorticity conservation in the shallow water equations, and see how this generalizes to a continuously stratified fluid.

In section 3.2 of the FFMC notes, an equation for the vertical vorticity of the rotating shallow water equations was formed by taking the curl of the shallow water momentum equations, giving

$$\zeta_t + u\zeta_x + v\zeta_y = -(\zeta + f)(u_x + v_y), \tag{2.1}$$

where $\zeta = v_x - u_y$ is the vertical component of the vorticity and $f$ is the Coriolis acceleration. In GFD, this is often referred to as the 'relative vorticity' to distinguish it from the 'planetary vorticity' ($f$) and the 'potential vorticity'. By combining Eq. (2.1) with an equation for the depth of the fluid, $H$,

$$H_t + (uH)_x + (vH)_y = 0 \quad \rightarrow \quad u_x + v_y = -\frac{1}{H}\frac{DH}{Dt}, \tag{2.2}$$

we arrived at a conservation equation

$$\frac{D}{Dt}\left(\frac{\zeta + f}{H}\right) = 0, \tag{2.3}$$

where $D/Dt = \partial_t + u\partial_x + v\partial_y$ is the material derivative. Eq. (2.3) is the shallow water PV conservation equation, and $(\zeta + f)/H$ is the shallow water PV. This equation was first derived by Carl-Gustav Rossby (Figure 5) in a paper in 1936 in which he used insights from laboratory experiments to help explain the dynamics of the Gulf Stream.

Eq. (2.3) states that the PV is a conserved tracer, that is it is constant following fluid parcels. In the absence of diffusion, passive tracers (like dye) would obey the same equation:

$$\frac{D}{Dt}C = 0. \tag{2.4}$$

Unlike passive tracers, however, the definition of PV involves the fluid velocity itself. Therefore Eq. (2.3) is a constraint on the fluid motion in a rotating system, in this case the rotating shallow water equations.

## 2.1 Ertel's Theorem

See Salmon §4.1

The PV conservation equation, Eq. (2.3) applies only under the shallow water approximation, namely a thin fluid with uniform density. We would like to obtain a similar expression that is more generally valid in the ocean and atmosphere. In this section, we will derive an equation for potential vorticity known as Ertel's theorem for the most general case first, and then examine some simplifying limits.

Start with the Navier-Stokes equations in a rotating coordinate frame

$$\frac{\partial \mathbf{u}}{\partial t} + \mathbf{u} \cdot \nabla \mathbf{u} + \mathbf{f} \times \mathbf{u} = -\frac{1}{\rho}\nabla p + \nu \nabla^2 \mathbf{u}, \tag{2.5}$$

$$\frac{\partial \rho}{\partial t} + \nabla \cdot (\rho \mathbf{u}) = 0. \tag{2.6}$$

To make the algebra easier later on, it is helpful to re-write the inertial term, $\mathbf{u} \cdot \nabla \mathbf{u}$ using the following vector identity

$$\nabla(\mathbf{A} \cdot \mathbf{B}) = (\mathbf{A} \cdot \nabla)\mathbf{B} + (\mathbf{B} \cdot \nabla)\mathbf{A} + \mathbf{A} \times (\nabla \times \mathbf{B}) + \mathbf{B} \times (\nabla \times \mathbf{A}). \tag{2.7}$$

Plugging in $\mathbf{A} = \mathbf{B} = \mathbf{u}$, we get

$$\mathbf{u} \cdot \nabla \mathbf{u} = \frac{1}{2}\nabla(\mathbf{u} \cdot \mathbf{u}) - \mathbf{u} \times \omega, \tag{2.8}$$

where $\omega \equiv \nabla \times \mathbf{u}$ is the vorticity. Using this expression, we can re-write Eq. (2.5)

$$\frac{\partial \mathbf{u}}{\partial t} + (\boldsymbol{\omega}_a) \times \mathbf{u} = -\frac{1}{\rho}\nabla p - \frac{1}{2}\nabla(\mathbf{u} \cdot \mathbf{u}) + \nu \nabla^2 \mathbf{u}. \tag{2.9}$$

where $\boldsymbol{\omega}_a \equiv \boldsymbol{\omega} + \mathbf{f}$ is the *absolute vorticity*. Just as we did for the shallow water equations, we can derive the vorticity equation by taking the curl of the momentum equation, i.e. $\nabla\times$ Eq. (2.9)

$$\frac{\partial \boldsymbol{\omega}}{\partial t} + \nabla \times (\boldsymbol{\omega}_a \times \mathbf{u}) = \nabla \left(\frac{1}{\rho}\right) \times \nabla p + \nu \nabla^2 \boldsymbol{\omega}. \tag{2.10}$$

The second term can be re-written using another vector identity:

$$\nabla \times (\mathbf{A} \times \mathbf{B}) = \mathbf{A}(\nabla \cdot \mathbf{B}) - \mathbf{B}(\nabla \cdot \mathbf{A}) + (\mathbf{B} \cdot \nabla)\mathbf{A} - (\mathbf{A} \cdot \nabla)\mathbf{B}, \tag{2.11}$$

and noting that the absolute vorticity can be written $\boldsymbol{\omega}_a = \nabla \times (\mathbf{u} + \Omega \times \mathbf{r})$ so that its curl is zero $\nabla \times \boldsymbol{\omega}_a = 0$. Since $\partial \mathbf{f}/\partial t = 0$ (over the timescales that we are interested in here, the Earth's rotation is constant) the vorticity equation can be re-written

$$\frac{D}{Dt}\boldsymbol{\omega}_a + \boldsymbol{\omega}_a(\nabla \cdot \mathbf{u}) = \boldsymbol{\omega}_a \cdot \nabla \mathbf{u} + \frac{1}{\rho^2}\nabla p \times \nabla \rho + \frac{\nu}{\rho}\nabla^2 \boldsymbol{\omega}. \tag{2.12}$$

where again, $D/Dt$ is the material derivative. The terms on the right hand side of Eq. (2.12) are familiar from non-rotating fluid mechanics; the first term is the vortex stretching/titling term, and the second

is the baroclinic torque. The divergence of the velocity field, $\nabla \cdot \mathbf{u}$, can be found from the continuity equation, (2.6):

$$\nabla \cdot \mathbf{u} = -\frac{1}{\rho}\frac{D\rho}{Dt}. \tag{2.13}$$

Then, notice that since

$$\frac{D}{Dt}\left(\frac{\boldsymbol{\omega}_a}{\rho}\right) = \frac{1}{\rho}\frac{D}{Dt}\boldsymbol{\omega}_a - \frac{1}{\rho^2}\boldsymbol{\omega}_a\frac{D\rho}{Dt}, \tag{2.14}$$

Eq. (2.12) can be further simplified by dividing by $\rho$ and collecting terms on the left hand side

$$\frac{D}{Dt}\left(\frac{\boldsymbol{\omega}_a}{\rho}\right) = \frac{\boldsymbol{\omega}_a}{\rho}\cdot\nabla\mathbf{u} + \frac{1}{\rho^3}\nabla p\times\nabla\rho + \frac{\nu}{\rho^2}\nabla^2\boldsymbol{\omega}. \tag{2.15}$$

Ertel's theorem combines this equation for the absolute vorticity with the evolution equation for an arbitrary passive scalar, $\lambda$:

$$\frac{D\lambda}{Dt} = S, \tag{2.16}$$

where $S$ represents sources and sinks of $\lambda$. We need to make one more step to combine the equation for $\lambda$ with the absolute vorticity. Taking the gradient of Eq. (2.16), and switching to index notation to keep track of the various gradient operators

$$\frac{D}{Dt}(\partial_i\lambda) = -(\partial_i u_j)\partial_j\lambda + \partial_i S. \tag{2.17}$$

Then, taking the dot product of the absolute vorticity $\boldsymbol{\omega}_a$ with Eq. (2.17),

$$\omega_i\frac{D}{Dt}(\partial_i\lambda) = \omega_i\partial_i S - \omega_i(\partial_i u_j)\partial_j\lambda, \tag{2.18}$$

or, back in vector notation,

$$\boldsymbol{\omega}_a\cdot\frac{D}{Dt}\nabla\lambda = \boldsymbol{\omega}_a\cdot\nabla S - [(\boldsymbol{\omega}_a\cdot\nabla)\,\mathbf{u}]\cdot\nabla\lambda. \tag{2.19}$$

Notice that the last term on the right hand side of Eq. (2.18) is the gradient of $\lambda$ dotted into the vortex stretching/tilting term. We can eliminate this term from the absolute vorticity equation by by dotting $\nabla\lambda$ into Eq. (2.15)

$$\boxed{\frac{D}{Dt}\left(\frac{\boldsymbol{\omega}_a\cdot\nabla\lambda}{\rho}\right) = \frac{1}{\rho^3}\nabla\lambda\cdot(\nabla\rho\times\nabla p) + \frac{\boldsymbol{\omega}_a}{\rho}\cdot\nabla S + \frac{\nu}{\rho}\nabla\lambda\cdot\nabla^2\boldsymbol{\omega}_a}. \tag{2.20}$$

This is the general form of Ertel's theorem, and $q \equiv (\boldsymbol{\omega}_a\cdot\nabla\lambda)/\rho$ is Ertel's potential vorticity (PV). This theorem was first derived in its most general form by Hans Ertel (Figure 5) in a 1942 paper called "a new hydrodynamic vorticity theorem" (in German).

Notice that we haven't specified what the scalar $\lambda$ is yet. Ertel's PV, $q$, can be defined for a variety of scalars. Common choices for $\lambda$ are the potential temperature in the atmosphere, and the potential density, or buoyancy in the ocean. If we neglect viscous effects, $\nu = 0$, and assume that $\lambda$ is conserved following the fluid ($S = 0$) and can be written as a function of pressure and density, $\lambda = \lambda(p, \rho)$, then

$$\boxed{\frac{D}{Dt}\left(\frac{\boldsymbol{\omega}_a\cdot\nabla\lambda}{\rho}\right) = 0}, \tag{2.21}$$

and the Ertel potential vorticity (Ertel PV),

$$q \equiv \frac{\boldsymbol{\omega}_a \cdot \nabla \lambda}{\rho}, \tag{2.22}$$

is conserved following fluid parcels.

The description so far hasn't shed much light on the physical description of potential vorticity. A more physical description of PV emerges when we consider a slight generalization of Ertel's PV. This discussion follows from Salmon §4.3.

Consider the PV in a homentropic fluid, where $\nabla\rho \times \nabla p = 0$. Let $\theta_1$, $\theta_2$, and $\theta_3$ be three passive scalars, each of which is conserved following the fluid:

$$\frac{D\theta_{1,2,3}}{Dt} = 0. \tag{2.23}$$

Further, assume that all three scalars are *independent*, that is none of their gradients are aligned anywhere in the flow, i.e.

$$\nabla\theta_1 \times \nabla\theta_2 \neq 0, \quad \nabla\theta_1 \times \nabla\theta_3 \neq 0, \quad \text{etc.} \tag{2.24}$$

We then have three different potential vorticity values, one corresponding to each scalar:

$$Q_{1,2,3} = \frac{\boldsymbol{\omega}_a \cdot \nabla\theta_{1,2,3}}{\rho}. \tag{2.25}$$

Since $\theta_{1,2,3}$ are independent, they form a generalized curvilinear coordinate basis, and since $D\theta_{1,2,3}/Dt = 0$, it is apparent that this coordinate system is *Lagrangian*. (For example, $\theta_{1,2,3}$ could be the $x, y, z$ locations of fluid particles at a given initial time.) For ease of notation, let's introduce the *absolute velocity*, $\mathbf{u}_a$, defined so that $\boldsymbol{\omega}_a = \nabla \times \mathbf{u}_a$. Let $\mathbf{A}$ be the absolute velocity components in the $\theta_{1,2,3}$ coordinate frame,

$$\mathbf{u}_a = A_1\nabla\theta_1 + A_2\nabla\theta_2 + A_3\nabla\theta_3. \tag{2.26}$$

The three potential vorticity values can be written out in index notation in terms of the absolute velocity:

$$Q_r = \frac{1}{\rho}\epsilon_{ijk}\frac{\partial u_k}{\partial x_j}\frac{\partial \theta_r}{\partial x_i}, \tag{2.27}$$

where $\epsilon_{ijk}$ is the Levi-Civita symbol, and we have dropped the subscript $a$ from the absolute velocity for notational clarity. From Eq. (2.26), the absolute velocity can be expressed in the $\theta_{1,2,3}$ coordinate frame:

$$u_k = A_s\frac{\partial \theta_s}{\partial x_k}, \tag{2.28}$$

and the PV components can be written

$$Q_r = \frac{1}{\rho}\epsilon_{ijk}\frac{\partial \theta_r}{\partial x_i}\frac{\partial \theta_s}{\partial x_k}\frac{\partial A_s}{\partial x_j}. \tag{2.29}$$

Expanding $\partial\theta_r/\partial x_i = (\partial\theta_r/\partial\theta_i)(\partial\theta_i/\partial x_i)$, and the same for index pair $s, k$, we get

$$Q_r = \frac{1}{\rho}\epsilon_{ijk}\frac{\partial \theta_r}{\partial \theta_i}\frac{\partial \theta_i}{\partial x_i}\frac{\partial \theta_s}{\partial \theta_k}\frac{\partial \theta_k}{\partial x_k}\frac{\partial A_s}{\partial \theta_j}\frac{\partial \theta_j}{\partial x_j}. \tag{2.30}$$

Since $\theta_{123}$ are independent, $\partial\theta_r/\partial\theta_i = \delta_{rj}$, where $\delta$ is the Kronecker delta. Furthermore, since $\theta_{123}$ are Lagrangian coordinates, the volume element in $\theta_{123}$ space must be equal to the volume element in $xyz$ space:

$$\frac{d\theta_1 d\theta_2 d\theta_3}{dxdydz} = 1. \tag{2.31}$$

Therefore, Eq. (2.30) can be written simply

$$Q_r = \frac{1}{\rho}\epsilon_{rjs}\frac{\partial A_s}{\partial\theta_j}, \tag{2.32}$$

or, in vector notation,

$$\mathbf{Q} = \frac{1}{\rho}\nabla_\theta \times \mathbf{A}, \tag{2.33}$$

where

$$\nabla_\theta \equiv (\frac{\partial}{\partial\theta_1}, \frac{\partial}{\partial\theta_2}, \frac{\partial}{\partial\theta_3}) \tag{2.34}$$

and potential vorticity conservation implies that

$$\frac{D}{Dt}\left(\frac{\nabla_\theta \times \mathbf{A}}{\rho}\right) = 0. \tag{2.35}$$

Eq. (2.33) gives us a physical interpretation of potential vorticity: It is the absolute vorticity, calculated in a Lagrangian coordinate frame. Note that $\mathbf{Q}$ is a vector, while the PV defined in Eq. (2.22) is a scalar. To recover the same expression in Eq. (2.22) from the above derivation, we would have to replace one of the $\theta$ coordinates by $\lambda$, which would then give

$$\frac{D}{Dt}\left[\frac{\nabla_\theta \times \mathbf{A}}{\rho}\cdot\nabla_\theta\lambda\right] = 0, \tag{2.36}$$

from which we see that the scalar Ertel PV is the component of $\mathbf{Q}$ directed along gradients in $\lambda$.

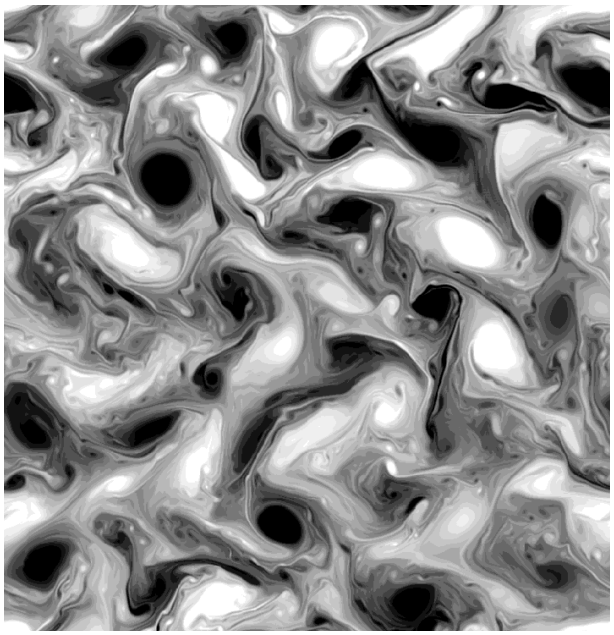

Figure 6: Temperature perturbations from a Quasi-Geostrophic model, in this case a variant called 'Surface QG'. Although the QG equations can be expressed in a very simple form, they contain many complex dynamical features including Rossby waves, geostrophic turbulence, zonal jets, etc. From Held et al. (1995) *J. Fluid Mech.* , **282**, 1-20.

# 3 Quasi-geostrophic dynamics

In the Fundamentals course, we derived the rotating shallow water equations by assuming that the horizontal scales of motion are much larger than the fluid depth, $H$. These equations can be written

$$u_t + uu_x + vu_y - fv = -g\eta_x, \tag{3.1}$$

$$v_t + uv_x + vv_y + fu = -g\eta_y, \tag{3.2}$$

$$h_t + (uh)_x + (vh)_y = 0, \tag{3.3}$$

where the fluid depth, $h$, is written in terms of the bottom depth, $H$, and free surface height, $\eta$: $h(x, y, t) = H(x, y) + \eta(x, y, t)$. We also derived an equation for the shallow water potential vorticity,

$$\frac{d}{dt}\left(\frac{\zeta + f}{h}\right) = 0. \tag{3.4}$$

This equation gives us physical insight into the constraints that rotation places on fluid motion, but it is not *predictive* since it is only one equation for three unknowns, $u$, $v$, and $\eta$. However, in a special limit which we will discuss, the PV conservation equation can be written as a prognostic equation for a single variable.

First, let's assume that the Rossby number, $Ro = U/fL$ is small. In this case the shallow water momentum equations are approximately

$$-fv = -g\eta_x, \tag{3.5}$$

$$fu = -g\eta_y, \tag{3.6}$$

and we can introduce a velocity streamfunction

$$\psi = g\eta/f. \tag{3.7}$$

The vertical vorticity and material derivative can also be written in terms of $\psi$

$$\zeta = \nabla \times \mathbf{u} = \nabla^2 \psi, \tag{3.8}$$

$$\frac{d}{dt} = \frac{\partial}{\partial t} - \frac{\partial \psi}{\partial y}\frac{\partial}{\partial x} + \frac{\partial \psi}{\partial x}\frac{\partial}{\partial y} = \frac{\partial}{\partial t} + J(\psi, \cdot) \tag{3.9}$$

The second simplification that we will make is the *beta-plane* approximation. So far, we have been considering the equations of motion in a cartesian coordinate frame centered at a given latitude, with the influence of the Earth's rotation represented by a constant rotation rate in the local vertical direction, the so-called $f$-plane approximation. We can obtain a more accurate approximation by expanding the Coriolis parameter in a Taylor series about the center of our coordinate frame ($y = 0$) at latitude $\theta$. Keeping the first two terms of the Taylor series

$$f \simeq f|_{y=0} + y \left.\frac{df}{dy}\right|_{y=0} = f_0 + \beta y, \tag{3.10}$$

where $f_0 = 2\Omega sin\theta$ is the vertical component of the rotation vector at $y = 0$, as before, and (in spherical coordinates)

$$\beta = \frac{1}{R}\frac{\partial f}{\partial \theta} = \frac{2\Omega cos\theta}{R}. \tag{3.11}$$

The form in Eq. (3.10) is called the *beta-plane* approximation. Consistent with keeping only the first two terms in the Taylor series expansion, we will explicitly assume that changes in the rotation rate are small over the scales of interest, i.e.

$$\beta L/f_0 << 1. \tag{3.12}$$

The third approximation is that fractional changes in the fluid depth are small, that is

$$h = H + \eta = H_0(1 + \frac{H - H_0}{H_0} + \frac{\eta}{H_0}), \tag{3.13}$$

where $H_0$ is a constant depth, and $H, \eta << H_0$. Combining these three assumptions, we can write an approximation to the shallow water PV in Eq. (3.4)

$$\frac{\zeta + f}{\eta + h} \simeq \frac{f_0\left(1 + \frac{\beta y}{f_0} + \frac{\zeta}{f_0}\right)}{H_0\left(1 + \frac{\eta}{H_0} + \frac{H - H_0}{H_0}\right)}. \tag{3.14}$$

Under our assumptions, each fractional term is small compared to 1, and the PV can be written

$$\frac{\zeta + f}{\eta + H} \simeq \frac{f_0}{H_0}\left(1 + \frac{\beta y}{f_0} + \frac{\zeta}{f_0} - \frac{\eta}{H_0} - \frac{H - H_0}{H_0}\right) \simeq \frac{f_0}{H_0}\left(1 + \frac{\beta y}{f_0} + \frac{\nabla^2 \psi}{f_0} - \frac{f_0 \psi}{g H_0} + \frac{H_0 - H}{H_0}\right). \tag{3.15}$$

Plugging this expression back into Eq. (3.4) gives the *Quasi-geostrophic equation*

$$\frac{\partial q}{\partial t} + J(\psi, q) = 0, \tag{3.16}$$

where $q$ is the quasi-geostrophic PV,

$$q \equiv \nabla^2\psi + f - \frac{f_0^2}{gH_0}\psi + f_0\frac{H_0 - H(x,y)}{H_0}. \tag{3.17}$$

The quasi-geostrophic (QG) equation is extremely useful because it is effectively one equation for a single unknown variable ($\psi$ and $q$ are related through Eq. 3.17.) To solve the equation numerically, we can time-step Eq. (3.16) to get $q$ at the new time step, and then solve Eq. (3.17) for the corresponding streamfunction. The QG equation is an important conceptual tool in dynamical meteorology and oceanography, and as we will see later, we can use it to reproduce many qualitative features of the ocean and atmosphere. As an example, Figure (6) shows the temperature field from a model solving a variant to the QG equations called the surface QG equation.

Finally, it is interactive to examine the relative sizes of two of the terms in Eq. (3.17), namely

$$q = \underbrace{\nabla^2\psi}_{(1)} - \underbrace{\frac{f_0^2}{gH_0}\psi}_{(2)} + \dots \tag{3.18}$$

If we condider the PV in Fourier space $\widehat{q}$, then

$$\widehat{q} = (k^2 + l^2)\widehat{\psi} - \frac{f_0^2}{gH_0}\widehat{\psi} + \dots \tag{3.19}$$

where $k$ and $l$ are the $x$ and $y$ wave numbers. From previous lectures, we recognize the *deformation scale*, $L_D = \sqrt{gH_0}/f_0$, and can define the corresponding wavenumber, $k_D \equiv L_D^{-1}$.

- Term (1) represents contributions from the relatively vorticity, $\zeta = \nabla^2\psi$ to the PV, and dominates at *small scales*, $|\mathbf{k}| >> k_D$.
- Term (2) represents contributions from changes in the surface height, $\eta = f\psi/g$, and dominates at *large scales*, $|\mathbf{k}| << k_D$.

In the next lecture, this observation will help us interpret the dynamics of large and small scale Rossby waves.

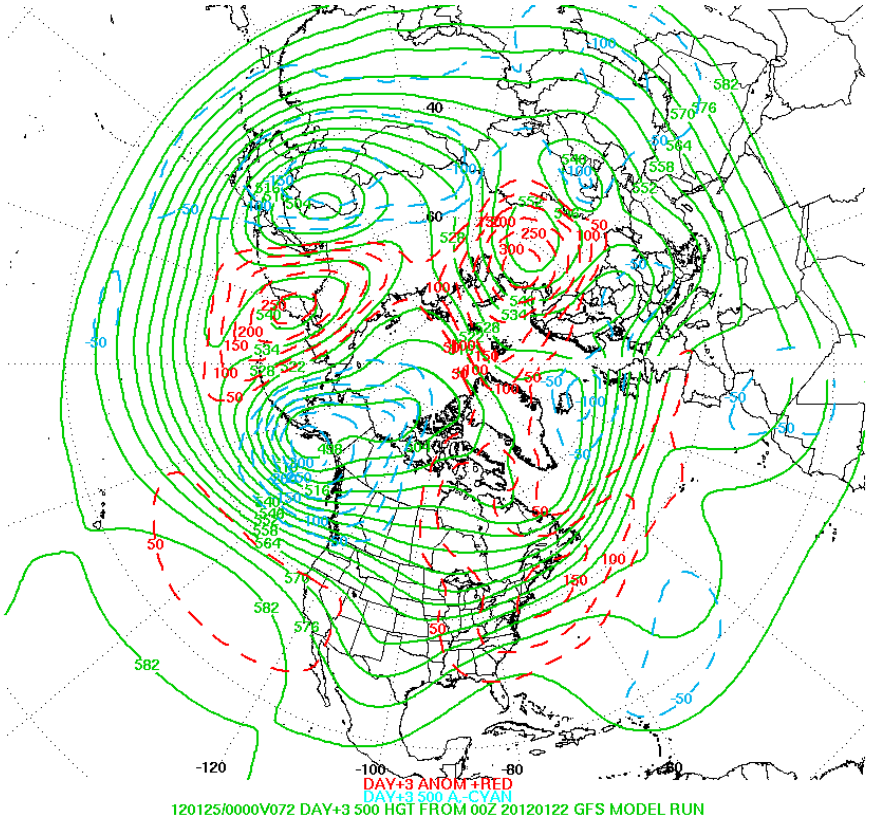


Figure 7: Forecast for the height of the 500mb pressure surface from the NCEP HPC model.

# 4 Rossby Waves

Rossby, or planetary, waves are very important and ubiquitous features of the ocean and atmosphere circulation. Figure 7 shows a model forecast for the height of the 500mb pressure surface. As we saw in the QG lecture, because the large-scale atmospheric circulation is close to geostrophic balance, the height contours act like a streamfunction. Although the flow at mid-latitudes is generally directed to the east, consistent with a thermal wind balance with the north/south temperature gradient, we see that the flow is highly distorted. These distortions are signatures of Rossby waves, which we experience everyday through changing weather patterns.

Here, we will first look at the waves supported by the QG equations. Recall from last time that these equations can be written:

$$\frac{\partial q}{\partial t} + J(\psi, q) = 0, \tag{4.1}$$

where $q$ is the quasi-geostrophic PV,

$$q \equiv \nabla^2 \psi + f - \frac{f_0^2}{g H_0}\psi + f_0 \frac{H_0 - H(x,y)}{H_0}. \tag{4.2}$$

Here, we will first make the assumption of a flat-bottom ($H = H_0$). We will also assume that the

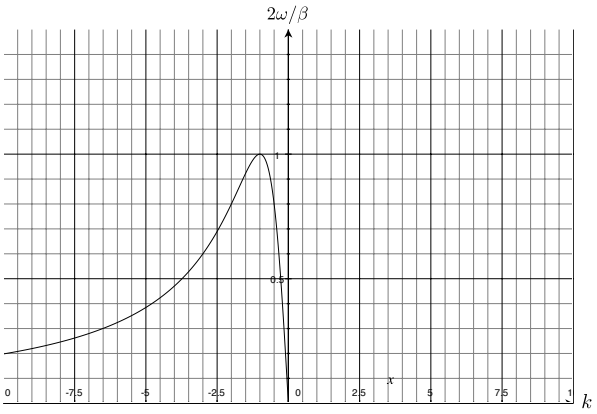


Figure 8: The Rossby wave dispersion relation (Eq. 4.7) with $l = 0$ and $k_D = 1$.

departures in the PV from the planetary vorticity ($f$) are small, and will linearize the QG equation. Assuming that $\eta$ and $\psi$ are small, and retaining only the leading order terms, the QG equation becomes

$$\frac{\partial q}{\partial t} + \beta \frac{\partial \psi}{\partial x} = 0, \tag{4.3}$$

or

$$\nabla^2 \psi_t - \frac{f_0^2}{g H_0} \psi_t + \beta \psi_x = 0. \tag{4.4}$$

Now, let's look for plane-wave solutions to this linearised QG equation of the form

$$\psi = \psi_0 e^{\imath(kx + ly - \omega t)}. \tag{4.5}$$

Plugging this form into Eq. (4.4) gives

$$(k^2 + l^2)\omega + k_D^2 \omega + k\beta = 0, \tag{4.6}$$

or

$$\omega = \frac{-k\beta}{k_D^2 + |\mathbf{k}|^2}, \tag{4.7}$$

where $k_D \equiv L_D^{-1} \equiv f_0/\sqrt{gH_0}$ is the inverse of the *deformation scale*. Eq. (4.7) is the *Rossby wave dispersion relation*.

The dispersion relation, Eq. (4.7), is plotted in Figure 8. The maximum possible frequency supported by the QG equations can be found from the Rossby wave dispersion relation by first setting $\partial\omega/\partial l = 0$ in Eq. (4.7):

$$\frac{\partial \omega}{\partial l} = \frac{2l\beta k}{k_D^2 + |\mathbf{k}|^2} = 0, \tag{4.8}$$

which implies that the fastest oscillating waves are independent of the $y$-direction, with $l = 0$. The maximum of $\omega$ with respect to $k$ is then

$$\frac{\partial \omega}{\partial k} = -\frac{\beta}{k_D^2 + |\mathbf{k}|^2} - \frac{2\beta k^2}{k_D^2 + |\mathbf{k}^2|} = 0, \tag{4.9}$$

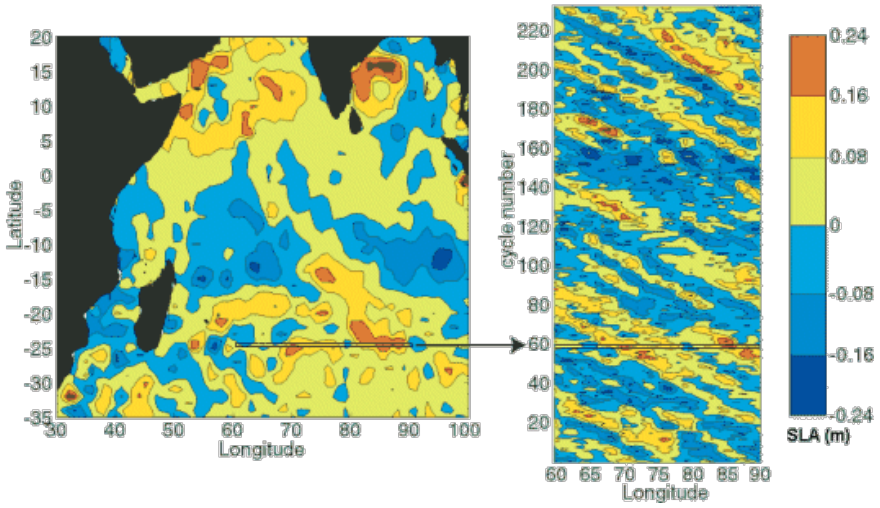


Figure 9: The westward phase propagation of Rossby waves in the ocean is clearly visible in a time-series of sea-surface height (SSH) anomalies from NASA's TOPEX/POSEIDON satellite, from Southampton Oceanography Centre. 10 cycles on the y-axis corresponds to about 3 months.

where $c \equiv \sqrt{gH_0}$. This simplifies to $k_D^2 + |\mathbf{k}|^2 - 2k^2 = 0$. If we consider waves with $l = 0$, we see that the maximum frequency therefore occurs at $k = -k_D$. Plugging this back into Eq. (4.7), the maximum frequency supported by the QG equations is

$$\omega_{\max} = \frac{\beta}{2k_D} = \frac{\beta\sqrt{gH_0}}{2f_0}. \tag{4.10}$$

Since $\beta = 2\Omega\cos\Theta/R$ and $f_0 = 2\Omega\sin\Theta$, where $\Theta$ is the latitude, $\Omega$ is the frequency of the Earth's rotation, and $R$ is the Earth's radius, the maximum frequency can be written

$$\omega_{\max}/f = \frac{\sqrt{gH_0}\tan\Theta}{2Rf}. \tag{4.11}$$

In the ocean, with $H_0 \simeq 4km$, and at a latitude of $45°$, $\omega_{\max} \simeq 0.16f$. Since $f$ is known as the *inertial frequency*, Rossby waves are always *sub-inertial*. Also, note that sub-inertial motions tend to be close to geostrophic balance since the Earth's rotation has plenty of time to take effect (although this was already obvious since we started our derivation by assuming that the Rossby number was small).

The zonal phase speed of the Rossby waves is

$$c_x = \frac{\omega}{k} = \frac{-\beta}{k_D^2 + |\mathbf{k}|^2}. \tag{4.12}$$

Since the denominator is positive, and $\beta \equiv \partial f/\partial y > 0$ for all latitudes (in both Hemispheres). Therefore, Rossby waves are characterized by *westward phase propagation.* Figure 9 shows clear evidence of the westward phase propagation of Rossby waves in the ocean.
We can gain some insight into the physical nature of Rossby waves by considering waves with large and small scales separately. First, let's consider small Rossby waves with $|\mathbf{k}|^2 >> k_D^2$. In this limit, Eq. (4.6)

becomes

$$(k^2 + l^2)\omega + k\beta \simeq 0. \tag{4.13}$$

If we look back through our derivation of the dispersion relation, we see that the first term in Eq. (4.13) came from the time rate of change of the relative vorticity, $\partial\zeta/\partial t$, while the second term came from the advection of planetary vorticity, $\beta\partial\psi/\partial x = v\partial f/\partial y$. Therefore, Eq. (4.13) is the dispersion relation corresponding to the following approximation:

$$\frac{D}{Dt}(\zeta + f) \simeq 0, \tag{4.14}$$

or

$$\frac{\partial\zeta}{\partial t} = -v\frac{\partial f}{\partial y}. \tag{4.15}$$

Imagine a large counter-clockwise rotating (cyclonic) eddy with $\zeta > 0$. The flow on the east side of the eddy moves north ($v > 0$), against the gradient in the planetary vorticity. Since $\partial f/\partial y > 0$, this leads to a decrease in $\zeta$. Conversely, the flow on the west side of the eddy moves south ($v < 0$), and leads to an increase in $\zeta$. Because the eddy itself is associated with positive vorticity ($\zeta > 0$), this results in a westward translation of the eddy.

The second limit is for large scale motions with $|\mathbf{k}|^2 << k_D^2$. This time, Eq. (4.6) is approximately

$$k_D^2\omega + k\beta \simeq 0. \tag{4.16}$$

Again, looking back through the derivation of the dispersion relation, we see that the first term came from the term involving changes in the surface elevation, $\partial\eta/\partial t$, so Eq. (4.16) is the dispersion relation corresponding to

$$\frac{D}{Dt}\left(\frac{f}{H}\right) \simeq 0, \tag{4.17}$$

or

$$\frac{\partial\eta}{\partial t} \simeq \frac{H}{f}v\frac{\partial f}{\partial y}. \tag{4.18}$$

Consider a localized east/west deformation in the surface height, with $\eta > 0$ at the bump, and $\eta = 0$ elsewhere. From geostrophic balance, $v = (\partial\eta/\partial x)/f$, so if we are in the Northern Hemisphere, $v > 0$ (northward flow) on the west side of the bump, and $v < 0$ (southward flow) on the east side of the bump. Eq. (4.18) tells us that the surface elevation will increase on the left side of the bump and decrease on the right side of the bump. Once again, this will result in the westward propagation of the bump.

## 4.1 Time-step constraints and the QG equation

As a brief aside, one significant advantage of the QG equation is that it greatly eases the computational burden compared to the full equations by filtering out internal gravity waves. The time step in numerical models of the ocean and atmosphere is often limited by the need to capture the fastest waves present in the system. Many ocean models, for example, use the 'rigid lid' approximation which removes surface gravity waves which propagate at very fast speeds, $c = \sqrt{gH}$. If we consider waves in water of depth $H = 4000$m (but sufficiently long wavelength that we can still use the shallow water phase speed), the waves propagate at $c \simeq 200$m/s! Even with a modest grid spacing of 10km, this restricts the time-step to no longer than 50s. A second practical stability constraint is that the resolved waves with the highest frequencies must be captured by the time-step of the model. Internal gravity waves present a further difficulty in this regard. For example, Figure 10 shows a cross-section of the measured buoyancy frequency,

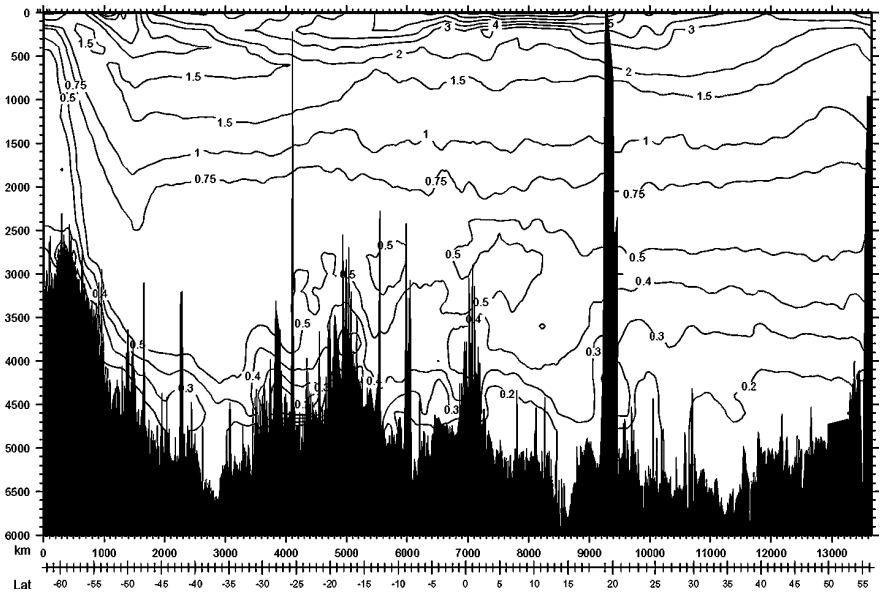


Figure 10: Cross-section of the buoyancy frequency in the ocean, contoured in units of cycles/hour, from Wunsch and Ferrari, Ann. Rev. Fluid Mech. (2004), **36**, 281-314.

$N$, in the ocean. Since internal waves can have frequencies up to $N$, the large values in the thermocline would effectively limit the time-step in a primitive equation model to at most 12 minutes. This is not as bad as the constraint based on surface gravity waves, but is still restrictive, especially for long simulations. For example, suppose that we wanted to run a climate simulation of the ocean/atmosphere system for 100 years. If we resolved internal waves with frequencies up to 5 cycles/hour, we would need more than 4 million time steps to complete our simulation!

The time-step constraint on the QG equations is much less stringent because these equations filter out internal gravity waves. We derived the maximum QG wave frequency in Eq. (4.10). Since $\beta = 2\Omega\cos\Theta/R$, and $f_0 = 2\Omega\sin\Theta$, where $\Theta$ is latitude, and $R$ is the radius of the Earth,

$$\omega_{\max} = \frac{\sqrt{gH_0}}{2R\tan\Theta}. \tag{4.19}$$

For an ocean with a maximum depth of about $H_0 = 4$km, at a latitude of 45°, the period of the fastest Rossby waves is about 4 days. This reduces the number of time steps required for our 100 year climate simulation to less than 10,000 - a very significant saving! Although QG models were very important to the development of numerical weather prediction, they are not commonly used operationally today. Instead, modelers have developed various tricks of filtering out the fastest gravity waves. Still, QG models remain very important tools in geophysical research.

## 4.2 Topographic Rossby Waves

In the derivation of the Rossby wave dispersion relation above, we neglected changes in the fluid depth, $H$. Rossby waves can also be supported by the PV gradient that accompanies changes in $H$, and these are

called 'topographic Rossby waves'. To see this, it is useful to consider the following laboratory experiment.

Suppose that we have a cylindrical tank of water, rotating about the $z$ axis with a rotation rate $\Omega$. We'll let it spin up until the fluid is in solid body rotation, that is $\mathbf{u} = 0$ in the rotating frame. The shallow water momentum equations then become

$$g\nabla H = \Omega^2 r\widehat{\mathbf{r}}, \tag{4.20}$$

where the new term on the right hand side is the centrifugal acceleration. The depth of the rotating fluid is then parabolic:

$$H = \frac{\Omega^2 r^2}{2g} + H_0. \tag{4.21}$$

Now, suppose that we change the rate of rotation by a small amount, $\Omega \rightarrow \Omega + \Delta\Omega$. Due to inertia, this will result in an apparent azimuthal velocity in the new rotating frame $(\Omega + \Delta\Omega)$ of $u_0 = -r\Delta\Omega$. Like we did on the rotating Earth, for convenience, we'll use cartesian coordinates with x pointing in the direction of rotation (westward) and y pointing towards the center of the tank (northward), so that $u_0 = y\Delta\Omega$. The streamfunction associated with this flow is

$$\psi_0 = \frac{-y^2\Delta\Omega}{2}. \tag{4.22}$$

Since the tank is rotating at a fixed rate, we don't have the beta effect, and $f = 2(\Omega + \Delta\Omega)$. The QG PV can then be written

$$q_0 = \nabla^2\psi_0 + f - k_D^2\psi_0 - \frac{f}{H_0}(H - H_0), \tag{4.23}$$

or

$$q_0 = -\Delta\Omega + 2(\Omega + \Delta\Omega) + k_D^2\frac{y^2\Delta\Omega}{2} - \frac{f\Omega^2 y^2}{2gH_0}. \tag{4.24}$$

If we assume that $\Delta\Omega << \Omega$, then this simplifies to

$$q_0 = 2\Omega - k_D^2\frac{y^2}{4}\Omega. \tag{4.25}$$

Now, let's consider linear perturbations to this base flow, $q = q_0 + q'$, $\mathbf{u} = \mathbf{u}_0 + \mathbf{u}'$, where $q' << q_0$ and $\mathbf{u}' << \mathbf{u}_0$. To leading order, the QG equation is

$$\frac{\partial q'}{\partial t} + u_0\frac{\partial q'}{\partial x} + v'\frac{\partial q_0}{\partial y} = 0, \tag{4.26}$$

where

$$q' = \nabla^2\psi' - k_d^2\psi', \tag{4.27}$$

and $v = \partial\psi'/\partial x$. To simplify the algebra, we will assume that $\partial q_0/\partial y$ is constant over the length scales of interest. This is equivalent to the $\beta$-plane approximation that we made in deriving the QG equations. As before, if we look for plane waves solutions of the form

$$\psi' = \widehat{\psi}e^{\imath(kx+ly-\omega t)}, \tag{4.28}$$

then we arrive at the following dispersion relation

$$\omega - ku_0 = \frac{-k(-k_D^2 y\Omega/2)}{|\mathbf{k}|^2 + k_D^2}. \tag{4.29}$$

There are two things to notice about this dispersion relation. First, when a mean flow is present, we see that the phase speed of the Rossby waves is only westward *relative to the mean flow*, $u_0$. This would have also been true for the flat-bottom planetary waves that we looked at earlier, had we included a mean flow in our analysis. This explains why mid-latitude weather systems still move to the east despite the fact that Rossby waves propagate westward (relative to the mean flow). Secondly, Eq. (4.29) has been written in a suggestive form, so that the right hand side would be identical to Eq. (4.7) if we replace $\beta$ with $\widehat{\beta}$ where

$$\widehat{\beta} = k_D^2 \frac{y\Omega}{2}. \tag{4.30}$$

This is what is known as the *effective beta*, or *topographic beta*, and emphasizes the very close analogy between gradients in the fluid depth and gradients in the planetary vorticity.
Now, suppose that we add a ridge to the bottom of the tank. As the mean flow moves over the ridge, it will excite Rossby waves. Since the topography is stationary in the rotating frame, the intrinsic frequency of the waves is $\omega = 0$. From Eq. (4.29), we see that the wavenumber of the excited waves is

$$|\mathbf{k}| = \left( -\frac{\widehat{\beta}}{u_0} - k_D^2 \right)^{1/2}. \tag{4.31}$$

Since $k_D = (2\Omega)^2/(gH)$, we can find the wavelength of the excited Rossby waves given the fluid depth and the rotation rates

$$\lambda \simeq k_D^{-1} \frac{\Delta\Omega}{\pi\Omega}. \tag{4.32}$$

Notice that the wavelength doesn't depend on the shape of the topography. Even a narrow ridge can excite large scale Rossby waves (so long as the flow around the ridge is still close to geostrophic balance).

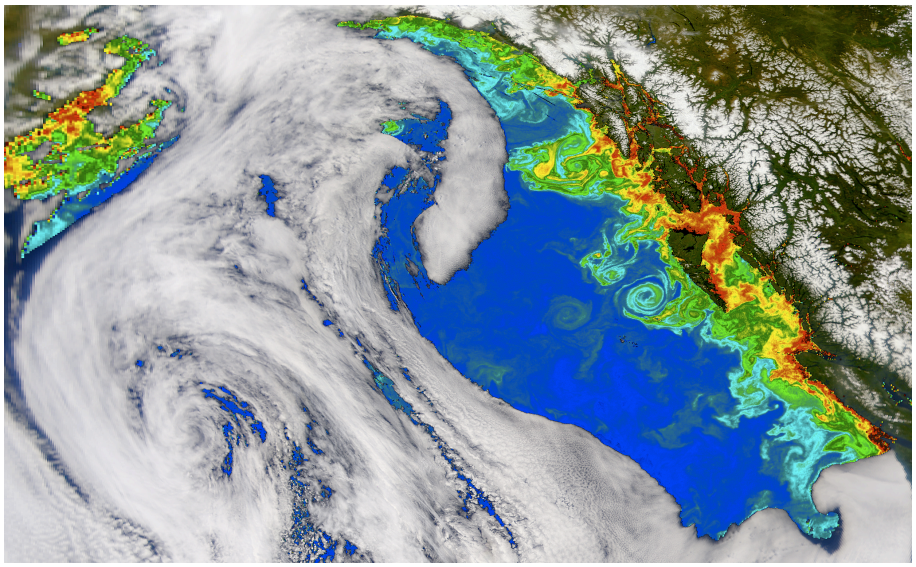

Figure 11: Eddies in the ocean and atmosphere

# 5 Baroclinic Instability

In the last lecture, we saw that Rossby waves are ubiquitous features of the ocean and atmosphere. However, the QG dispersion relation can support Rossby waves of any scale. Why do we see eddies in the ocean and atmosphere on very characteristic scales? In particular, why are the storm systems in the atmosphere much larger than the 'mesoscale' eddies in the ocean (see Figure 11)? In this section, we will show that these eddies are generated by baroclinic instability.

As we will see later, baroclinic instability requires available potential energy, and as it develops, converts potential energy into kinetic energy. Because of this, we cannot capture baroclinic instability in the one-layer QG equation that we derived two lectures ago. Instead, let's go back to the rotating Navier-Stokes equations, neglecting friction and diabetic effects, and assuming the fluid is in hydrostatic balance. The case that we will look at is known as the *Eady problem*, which was first derived by Eric Eady.

$$\frac{\partial \mathbf{u}}{\partial t} + \mathbf{u} \cdot \nabla \mathbf{u} + \mathbf{f} \times \mathbf{u} = -\nabla p, \tag{5.1}$$

$$\frac{\partial p}{\partial z} = b, \tag{5.2}$$

$$\nabla \cdot \mathbf{u} = 0, \tag{5.3}$$

$$\frac{\partial b}{\partial t} + \mathbf{u} \cdot \nabla b = 0. \tag{5.4}$$

The boundary conditions that we will apply are to this system are

$$w = 0, \quad @ \quad z = -H, H. \tag{5.5}$$

In the context of the atmosphere, we can think of the lower boundary as the ground and the top boundary as the tropopause, and we will assume that both surfaces are flat. (Using $z = -H$ as the position of the

lower boundary instead of the usual $z = 0$ is a trick to allow us to exploit the symmetry in the problem later on.)

Let's consider a base state with constant buoyancy gradients in the $y$ and $z$ direction, and a mean flow in the $x$ direction:

$$\mathbf{u} = \overline{u}(z)\hat{i} + \mathbf{u}'(x, y, z, t), \tag{5.6}$$
$$b = \overline{b}(y, z) + b'(x, y, z, t), \tag{5.7}$$
$$p = \overline{p}(y, z) + p'(x, y, z, t), \tag{5.8}$$

where the perturbations are small compared to the base state, i.e. $u' << \overline{u}$, etc. The base state then satisfies

$$f\overline{u}_z = -\overline{p}_{yz} = -\overline{b}_y \equiv -M^2, \tag{5.9}$$

where $M^2 \equiv \partial\overline{b}/\partial y$ is the horizontal analogue of the buoyancy frequency, $N$. Then, linearizing the equations about the base state,

$$u'_t + \overline{u}u'_x - fv' = -p'_x, \tag{5.10}$$
$$v'_t + \overline{u}v'_x + fu' = -p'_y, \tag{5.11}$$
$$u'_x + v'_y + w'_z = 0, \tag{5.12}$$
$$p'_z = b', \tag{5.13}$$
$$b'_t + \overline{u}b'_x + v'\overline{b}_y + w'\overline{b}_z = 0. \tag{5.14}$$

Taking the curl of the perturbation momentum equations

$$(\partial_t + \overline{u}\partial_x)\zeta' + f(u'_x + v'_y) = 0. \tag{5.15}$$

We will further assume that the *perturbation* quantities are geostrophic, with $Ro' \equiv u'/(fL) << 1$, in which case

$$f\zeta' = \nabla^2 p'. \tag{5.16}$$

Using this expression in Eq. (5.15), with $-w'_z = u'_x + v'_y$ gives

$$(\partial_t + \overline{u}\partial_x)\nabla^2 p'/f - fw'_z = 0. \tag{5.17}$$

Returning to the perturbation buoyancy equation, and using $v' = p'_x/f$ and $b' = p'_z$,

$$(\partial_t + \overline{u}\partial_x)p'_z + p'_x\frac{M^2}{f} + w'N^2 = 0, \tag{5.18}$$

or, taking $\partial/\partial z$

$$(\partial_t + \overline{u}\partial_x)p'_{zz} = -N^2 w'_z, \tag{5.19}$$

noting that the last two terms on the left hand side cancel since $d\overline{u}/dz = -M^2/f$ by the thermal wind relation. Using this expression in Eq. (5.17), we get

$$(\partial_t + \overline{u}\partial_x)(\nabla^2 p' + \frac{f^2}{N^2}p'_{zz}) = 0. \tag{5.20}$$

Since we can define a streamfunction, $\psi' = p'/f$, this equation is a linearized version of what is known as the 'stratified QG' equation:

$$\frac{\partial q}{\partial t} + J(\psi, q) = 0, \tag{5.21}$$
$$q = \nabla^2\psi + f + \frac{\partial}{\partial z}\left(\frac{f^2}{N^2}\frac{\partial\psi}{\partial z}\right). \tag{5.22}$$

Also notice that Eq. (5.20) would be an isotropic Laplacian if the vertical coordinate were re-scaled by $N/f$, which is known as the *Prandtl* ratio, which is an important parameter in ocean/atmosphere dynamics.

We will now look for normal mode solutions to Eq. (5.20) of the form

$$p' = \hat{p}(z)e^{ik(x-ct)+ily}. \tag{5.23}$$

The equation for the eigenvector, $\hat{p}$ is

$$-(k^2+l^2)\hat{p} + \frac{f^2}{N^2}\hat{p}_{zz} = 0, \tag{5.24}$$

or

$$\hat{p}_{zz} - \alpha^2\hat{p} = 0, \tag{5.25}$$

where $\alpha \equiv (N/f)|\mathbf{k}|$. Solutions to Eq. (5.25) take the form

$$\hat{p} = A\cosh(\alpha z) + B\sinh(\alpha z). \tag{5.26}$$

To proceed further, we need to use the boundary conditions of no normal flow at the top and bottom surface:

$$w = 0, \quad @ \quad z = -H, \quad z = H. \tag{5.27}$$

We need to relate these boundary conditions to the pressure to solve Eq. (5.20), and to do this, we can use the perturbation buoyancy equation, Eq. (5.18). Setting $w = 0$ implies

$$(\partial_t + \overline{u}\partial_x)p'_z - \frac{dU}{dz}p'_x = 0, \quad @ \quad z = -H, H, \tag{5.28}$$

where $dU/dz = -M^2/f$. Using Eq. (5.23) in this equation gives

$$\alpha(\overline{u}-c)\left(A\sinh(\alpha z) + B\cosh(\alpha z)\right) - \frac{dU}{dz}\left(A\cosh(\alpha z) + B\sinh(\alpha z)\right) = 0. \tag{5.29}$$

At the lower boundary, $\overline{u} = z(dU/dz) = -H(dU/dz)$, so the boundary condition can be written

$$\alpha(H\frac{dU}{dz} + c)\left(-A\sinh(\alpha z) + B\cosh(\alpha z)\right) + \frac{dU}{dz}\left(A\cosh(\alpha z) - B\sinh(\alpha z)\right) = 0, \tag{5.30}$$

where we have used the fact that $\sinh(-x) = -\sinh(x)$ and $\cosh(-x) = \cosh(x)$. Now, we can exploit the symmetry in the problem by separating the terms of Eq. (5.30) that are even and odd with respect to $H$, to give the following two equations

$$-\alpha H\frac{dU}{dz}A\sinh(\alpha H) + \alpha cB\cosh(\alpha H) + A\frac{dU}{dz}\cosh(\alpha H) = 0, \tag{5.31}$$

$$-\alpha cA\sinh(\alpha H) + \alpha H\frac{dU}{dz}B\cosh(\alpha H) - B\frac{dU}{dz}\sinh(\alpha H) = 0. \tag{5.32}$$

Dividing the first equation by $\cosh(\alpha H)$, and the second by $\sinh(\alpha H)$ gives

$$\frac{dU}{dz}A(-\alpha H\tanh(\alpha H) + 1) + \alpha cB = 0, \tag{5.33}$$

$$-\alpha cA + \frac{dU}{dz}B(\alpha H\coth(\alpha H) - 1) = 0. \tag{5.34}$$

In order for non-trivial solutions to exist, the determinant of the coefficient matrix must be equal to zero,

$$\begin{vmatrix} \frac{dU}{dz}(-\alpha H\tanh(\alpha H)+1) & \alpha c \\ -\alpha c & \frac{dU}{dz}(\alpha H\coth(\alpha H)-1) \end{vmatrix} = 0 \tag{5.35}$$

or

$$c^2 = H^2\left(\frac{dU}{dz}\right)^2\left(\tanh(\alpha H)-\frac{1}{\alpha H}\right)\left(\coth(\alpha H)-\frac{1}{\alpha H}\right). \tag{5.36}$$

In order to have unstable solutions, $c$ must have an imaginary part, i.e. $c^2 < 0$. However, $\cosh(x)-1/x > 0$ for all $x > 0$, so our stability criteria is simply

$$\tanh(\alpha H)-\frac{1}{\alpha H} < 0. \tag{5.37}$$

Eq. (5.36) is plotted in Figure (12). The maximum growth rate occurs for $\alpha H \simeq 0.8$. Recall that $\alpha \equiv N|\mathbf{k}|/f$, so the most unstable wavenumber is

$$|\mathbf{k}| \simeq 0.8\frac{f}{NH} = 0.8k_I, \tag{5.38}$$

where $k_I = L_I^{-1}$, and $L_I^{-1}$ is the *internal deformation scale*. Finally, let's take a look at some typical values in the ocean and atmosphere. First, for the atmosphere,

$$N \sim 4\times 10^{-2}s^{-1}, \tag{5.39}$$
$$f \sim 1\times 10^{-4}s^{-1}, \tag{5.40}$$
$$H \sim 10km, \tag{5.41}$$

which implies that $L_I \simeq 4000km$. For the ocean,

$$N \sim 4\times 10^{-3}s^{-1}, \tag{5.42}$$
$$f \sim 1\times 10^{-4}s^{-1}, \tag{5.43}$$
$$H \sim 4km, \tag{5.44}$$

and $L_I \simeq 160km$. These scales are in good agreement with the structures that we saw in Figure 11, and explain why synoptic scales in the atmosphere are significantly larger than those in the ocean.

## 5.1 Energetics

To see the energy source for baroclinic instability, let's look at the aspect ratio of the motions that develop. Specifically, let's compare the ratio of the vertical to horizontal velocity and the isopycnal slope,

$$\frac{w}{u} \sim r^2\frac{M^2}{N^2}. \tag{5.45}$$

When $r < 1$, the motions will tend to lie on surfaces that are shallower than the isopycnal slope, and when $r > 1$, the motion will be steeper than the isopycnal slope. Recall that from the vorticity equation, Eq. (5.15), we have

$$(\partial_t + \overline{u}\partial_x)\zeta = -fw_z. \tag{5.46}$$

This implies that based on characteristic horizontal and vertical length scales, $L$, and $H$,

$$\frac{U^2}{L^2} \sim f\frac{W}{H}. \tag{5.47}$$

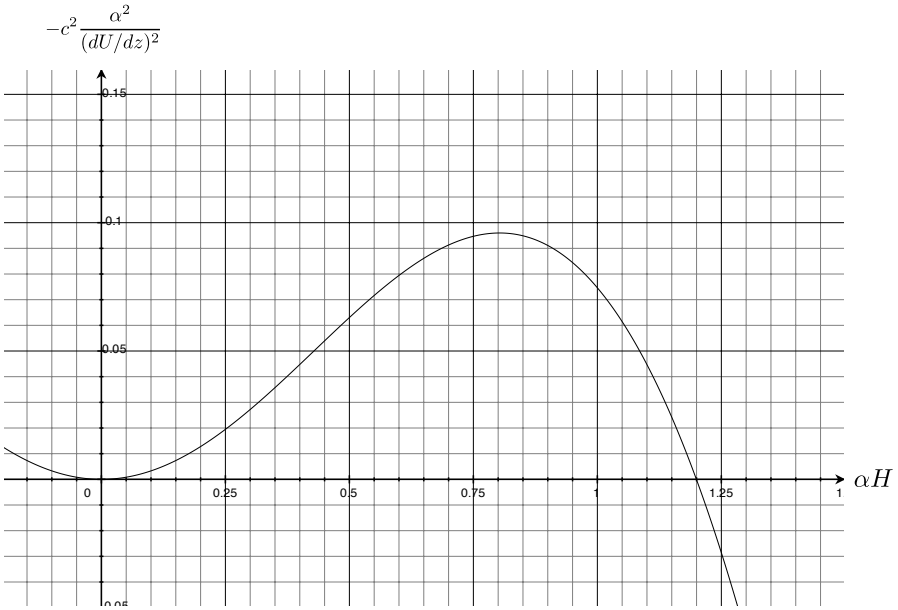


Figure 12: The baroclinic instability growth rate, rescaled from Eq. (5.36).

If we assume that the horizontal velocity, $U$, scales with $d\overline{u}/dzH$, then from the thermal wind relation

$$U \sim \frac{M^2}{f} H, \tag{5.48}$$

and

$$\frac{W}{U} \sim \frac{H^2}{f}\frac{M^2}{fL^2}. \tag{5.49}$$

Comparing this with Eq. (5.45), we see that

$$L^2 \sim \frac{1}{r^2}\frac{N^2H^2}{f^2}, \tag{5.50}$$

or

$$L \sim \frac{1}{r} L_I \tag{5.51}$$

where, again $L_I \equiv NH/f$ is the internal deformation scale. Since our criteria for baroclinic instability is that

$$L \gtrsim L_I, \tag{5.52}$$

the induced motion will generally have $r < 1$, taking shallower trajectories than the isopycnals. This implies that fluid moving up will have lower density than the surrounding fluid, and downward moving fluid will tend to be heavier than the neighboring fluid. On average, the buoyancy flux, $\overline{w'b'} > 0$, will therefore be positive, and energy will be transferred from potential to kinetic energy. Baroclinic instability grows at the expense of the available potential energy associated with the basic state. This means that baroclinic instability is not possible when the isopycnal surfaces are flat, $M^2/N^2 = 0$, and the available potential energy is also zero.

We can also think about the relation between the potential energy release and the stability criteria in reverse. We saw from our analysis of the Eady problem that the flow was only unstable to large scale perturbations (with $|\mathbf{k}|$ less than some cutoff). Now we can see why this is the case. For scales much smaller than the deformation scale, $L << L_I$, Eq. (5.51) implies that $r >> 1$, and fluid particles will move along trajectories much steeper than the isopycnals. However, in this case, heavy fluid will have to rise and light fluid will move down, $\overline{w'b'} < 0$, and the flow will lose kinetic energy to the potential energy field. This qualitatively explains why small scales are not unstable to baroclinic instability.

As we saw, baroclinic instability in the Eady problem depends strongly on the boundary condition. In fact, our stability criteria came directly from applying the boundary condition through the buoyancy equation. In a more general sense, baroclinic instability can also arise when gradients in the potential vorticity exist in the interior of the fluid (in the Eady problem, the interior PV is constant.) The second famous demonstration of baroclinic instability was discovered by Jule Charney (working independently of Eady) and is now called the 'Charney problem'. Unlike Eady, Charney allowed $f$ vary with latitude, which generates a gradient in the PV. A very useful criteria for baroclinic instability (see Gill §13.5) is that the following three functions must not have the same sign everywhere:

$$\partial\overline{q}/\partial y, \quad \partial\overline{b}/\partial y|_{bottom}, \quad -\partial\overline{b}/\partial y|_{top}, \tag{5.53}$$

where $\overline{q}$ and $\overline{b}$ are the PV and buoyancy associated with the basic state.

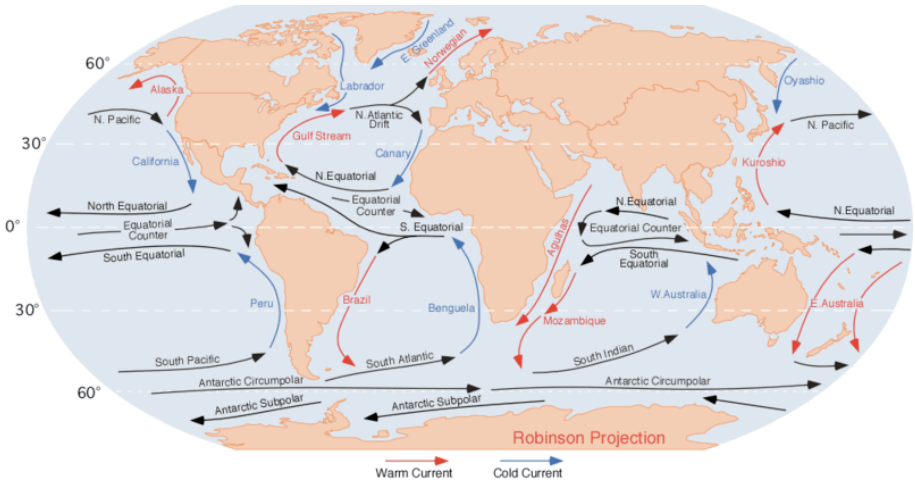


Figure 13: Major ocean current systems

# 6 Ocean circulation

See Salmon, §3.4

Now that we have a picture of the atmospheric circulation, we are in a position to understand some important features of the large-scale ocean circulation. To a large degree, the ocean circulation driven by wind. At the same time, the oceans are able to store vast quantities of heat and carbon. Therefore, the earth's climate depends strongly on the coupling between the dynamical coupling between the ocean and atmosphere.

With the notable of the Southern Ocean, the oceans are bounded by continents, preventing global zonal currents. Instead, looking at a map of ocean currents like that in Figure 13, we see that the ocean circulation is composed of a number of large-scale re-circulation patterns, or *gyres*. These gyres can be explained by the pattern of atmospheric forcing that we saw earlier. By solving for the circulation associated with the ocean gyres, we will also uncover an early puzzle in physical oceanography: why do strong boundary currents like the Gulf Stream form only on the western edges of ocean basins?

Consider the flow in an idealized rectangular basin, of width $L$, shown in the schematic of Figure 14. We will apply no-slip and no normal flow boundary conditions at all lateral boundaries. Also, assume that the bottom of the ocean is flat, at $z = -H$ with $H$ constant. We will invoke what is known as the rigid-lid approximation, and assume that the vertical velocity vanishes at the top and bottom boundaries, $w = 0$, @ $z = 0$ and $z = -H$. As before, we will assume that the Rossby number is small. However, now we need to keep the frictional terms, since the flow is driven by the wind stress at the ocean surface. Assuming the the flow is also incompressible, we have

$$\mathbf{f} \times \mathbf{u} = -\nabla p + \nu \nabla_h^2 \mathbf{u} + \nu \mathbf{u}_{zz}, \tag{6.1}$$

$$\nabla \cdot \mathbf{u} = 0, \tag{6.2}$$

where we have split the viscous term into the horizontal and vertical components, and $\nabla_h^2 \equiv \partial_x^2 + \partial_y^2$. Integrate these equations throughout the full depth of the ocean, from $z = -H$ to $z = 0$. From Eq. (6.2),

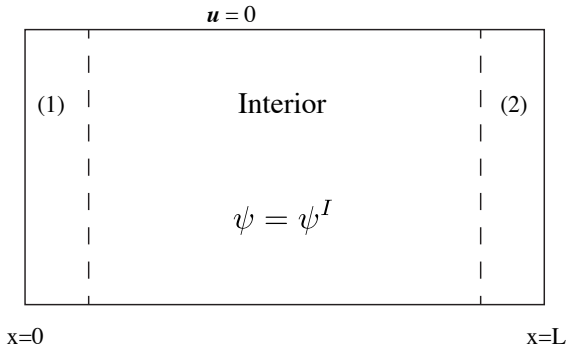


Figure 14: Sketch of our solution domain

since $w(z = 0, -H) = 0$, we have

$$\nabla \cdot \overline{\mathbf{u}} = 0, \tag{6.3}$$

where $\overline{\mathbf{u}} = (\overline{u}, \overline{v}, 0)$ is the depth-integrated flow. The depth-integrated momentum equation is

$$\mathbf{f} \times \overline{\mathbf{u}} = -\nabla \overline{p} + \nu \nabla_h^2 \overline{\mathbf{u}} + \nu \left. \frac{\partial \overline{\mathbf{u}}}{\partial z} \right|_{-H}^{0}. \tag{6.4}$$

The last term on the right hand side represents the stress at the top and bottom of the ocean, i.e.

$$\boldsymbol{\tau}^w = \nu \left. \frac{\partial \overline{\mathbf{u}}}{\partial z} \right|_0, \quad \boldsymbol{\tau}^b = \nu \left. \frac{\partial \overline{\mathbf{u}}}{\partial z} \right|_{-H}, \tag{6.5}$$

where $\boldsymbol{\tau}^w$ and $\boldsymbol{\tau}^b$ are the wind and bottom stress. Here, we will assume that $\boldsymbol{\tau}^b << \boldsymbol{\tau}^w$ and neglect the bottom stress. Taking the curl of Eq. (6.4) and using the vector identities

$$\nabla \times (\mathbf{A} \times \mathbf{B}) = \mathbf{A}(\nabla \cdot \mathbf{B}) - \mathbf{B}(\nabla \cdot \mathbf{A}) + \mathbf{B} \cdot \nabla \mathbf{A} - \mathbf{A} \cdot \nabla \mathbf{B}, \tag{6.6}$$

$$\nabla \times (\nabla \mathbf{A}) = 0, \tag{6.7}$$

gives

$$\mathbf{f}(\nabla \cdot \overline{\mathbf{u}}) - \overline{\mathbf{u}}(\nabla \cdot \mathbf{f}) + \overline{\mathbf{u}} \cdot \nabla \mathbf{f} - \mathbf{f} \cdot \nabla \overline{\mathbf{u}} = \nu \nabla^2 \overline{\boldsymbol{\omega}} + \nabla \times \boldsymbol{\tau}^w. \tag{6.8}$$

If we use the 'traditional approximation', and retain only the vertical component of $\mathbf{f}$, so that $\mathbf{f} = f(y)\hat{k}$, then this equation simplifies significantly. Noting that

$$\nabla \cdot \overline{\mathbf{u}} = 0, \tag{6.9}$$

$$\overline{w} = 0, \tag{6.10}$$

$$\nabla \cdot \mathbf{f} = 0, \tag{6.11}$$

$$\mathbf{f} \cdot \nabla \overline{\mathbf{u}} = 0, \tag{6.12}$$

Eq. (6.8) becomes

$$\overline{\mathbf{u}} \cdot \nabla \mathbf{f} = \nu \nabla^2 \overline{\boldsymbol{\omega}} + \nabla \times \boldsymbol{\tau}^w. \tag{6.13}$$

Note that while this is a vector equation, only the vertical component of each term is non-zero. In the limit when the horizontal friction term is unimportant, we have simply

$$\beta \overline{v} = W, \tag{6.14}$$

where $W$ is the vertical component of the wind stress curl, $W \equiv (\nabla \times \boldsymbol{\tau}^w) \cdot \hat{\mathbf{k}}$. Eq. (6.14) is known as *Sverdrup flow*. This implies that a negative wind stress curl (such as that found between the westerlies and trade winds) will result in an equatorward flow. It is useful to introduce a streamfunction $\psi$ associated with the depth-integrated flow, so that $\overline{\mathbf{u}} = -\nabla \times \psi$. Then, noting that

$$\nabla \times \nabla \times \mathbf{A} = \nabla(\nabla \cdot \mathbf{A}) - \nabla^2 \mathbf{A}, \tag{6.15}$$

the relative vorticity is

$$\boldsymbol{\omega} = \nabla \times \overline{\mathbf{u}} = \nabla \times (-\nabla \times \psi) = -\nabla(\nabla \cdot \psi) + \nabla^2 \psi = \nabla^2 \psi, \tag{6.16}$$

and the vertical component of Eq. (6.13) becomes

$$\beta \psi_x = \nu \nabla^4 \psi + W. \tag{6.17}$$

Eq. (6.14) then becomes

$$\beta \psi_x = W. \tag{6.18}$$

Assuming that the wind stress curl is a function of $y$ only, $W = W(y)$, the streamfunction is

$$\psi = x \frac{W}{\beta} + G(y). \tag{6.19}$$

where $G(y)$ is a function to be determined from applying the boundary conditions. Remember that our boundary conditions are that $\overline{\mathbf{u}} = 0$ at all boundaries. Because this amounts to setting $\psi_x = 0$ *and* $\psi_y = 0$, we have a problem: for an arbitrary wind field, we cannot satisfy both boundary conditions with the single function $G(y)$! For example, at $x = 0$, our boundary conditions require that

$$\psi_x = \frac{W}{\beta} = 0, \tag{6.20}$$

but this is only true for the trivial case when $W = 0$. This implies that Eq. (6.18) can't hold throughout the domain, and we must have *boundary layers* where the horizontal friction terms play a role and allow the solution to satisfy the boundary conditions.

To solve the full problem in Eq. (6.17), we will use boundary layer theory, specifically, the *method of undetermined coefficients*. First, let's consider just the east and west boundaries at $x = 0$ and $x = L$. This analysis will help explain why western boundary currents are so much stronger than eastern boundary currents.

Consider a domain like the one shown in Figure 14. Write the full solution as the combination of the solution in the interior, plus corrections in the east/west boundary layers:

$$\psi = \psi^I + \widetilde{\psi}^{(1)} + \widetilde{\psi}^{(2)}. \tag{6.21}$$

Because the horizontal friction term is negligible in the interior, the interior solution, $\psi^I$, is just Eq. (6.19)

$$\psi^I = x \frac{W(y)}{\beta} + G(y). \tag{6.22}$$

First, let's consider region (1) in the western boundary layer. Here, we will rescale the $x$ coordinate by the viscosity, which we assume to be small, $\epsilon = \nu$. Since we don't know how thin the boundary layer

should be, we will rescale $x$ by $\epsilon^a$, where $a$ is to be determined based on the dominant balance. Inside the western boundary layer, Eq. (**??**) then becomes

$$\beta\psi_x^I + \beta\widetilde{\psi}_{\widetilde{x}}^{(1)} = \epsilon\widetilde{\psi}_{\widetilde{x}\widetilde{x}\widetilde{x}\widetilde{x}}^{(1)} + W(y), \tag{6.23}$$

or

$$\beta\widetilde{\psi}_{\widetilde{x}}^{(1)} = \epsilon\widetilde{\psi}_{\widetilde{x}\widetilde{x}\widetilde{x}\widetilde{x}}^{(1)}, \tag{6.24}$$

where the rescaled coordinate is

$$\widetilde{x} = \frac{x}{\epsilon^a}. \tag{6.25}$$

In order to recover the interior solution outside the boundary layer, we require that

$$\widetilde{\psi} \to 0, \quad \text{as} \quad \widetilde{x} \to \infty. \tag{6.26}$$

Substituting Eqns. (6.21) and (6.25) into Eq. (6.17) gives

$$\beta\epsilon^{-a}\widetilde{\psi}_{\widetilde{x}}^{(1)} = \epsilon^{1-4a}\widetilde{\psi}_{\widetilde{x}\widetilde{x}\widetilde{x}\widetilde{x}}^{(1)}. \tag{6.27}$$

From this equation, we see that the dominant balance inside the boundary layer is between the advection of planetary vorticity (LHS) and lateral friction (RHS). In order to achieve this balance, we need to match the powers of $\epsilon$ so that

$$-a = 1 - 4a, \tag{6.28}$$

or $a = 1/3$. Our equation for the boundary layer correction is then

$$\widetilde{\psi}_{\widetilde{x}}^{(1)} = \beta^{-1}\widetilde{\psi}_{\widetilde{x}\widetilde{x}\widetilde{x}\widetilde{x}}^{(1)}. \tag{6.29}$$

Since this is a homogeneous, ODE with constant coefficients, we look for solutions of the form

$$\widetilde{\psi} = e^{r\widetilde{x}}. \tag{6.30}$$

Using this form in Eq. (6.29) gives

$$r^4 - \beta r = 0. \tag{6.31}$$

One root to this equation is $r = 0$, leaving

$$r^3 = \beta. \tag{6.32}$$

The roots to this equation lie on a circle of radius $\beta^{1/3}$ in the complex plane with angles $\theta = 0, 2\pi/3, -2\pi/3$, or

$$r = \beta^{1/3} \tag{6.33}$$

$$r = \beta^{1/3}cos(2\pi/3) + i\beta^{1/3}sin(2\pi/3) = -\frac{1}{2}\beta^{1/3} + i\frac{\sqrt{3}}{2}\beta^{1/3}, \tag{6.34}$$

$$r = \beta^{1/3}cos(-2\pi/3) + i\beta^{1/3}sin(-2\pi/3) = -\frac{1}{2}\beta^{1/3} - i\frac{\sqrt{3}}{2}\beta^{1/3}. \tag{6.35}$$

The general solution is then

$$\widetilde{\psi}^{(1)} = A(y) + B(y)e^{\beta^{1/3}\widetilde{x}} + C(y)e^{-\beta^{1/3}\widetilde{x}/2}e^{i\beta^{1/3}\widetilde{x}\sqrt{3}/2} + D(y)e^{-\beta^{1/3}\widetilde{x}/2}e^{-i\beta^{1/3}\widetilde{x}\sqrt{3}/2}. \tag{6.36}$$

Since we require that $\widetilde{\psi}$ vanishes in the interior for $\widetilde{x} \to \infty$, we need $A(y) = B(y) = 0$. For convenience, let's also re-write the last two constants in amplitude/phase form

$$\widetilde{\psi}^{(1)} = C(y)e^{-\beta^{1/3}\widetilde{x}/2}cos\left(\frac{\sqrt{3}}{2}\beta^{1/3}\widetilde{x} + D(y)\right). \tag{6.37}$$

Now, we need to select $C(y)$ and $D(y)$ to meet the boundary conditions. Recall that we want $\overline{\mathbf{u}} = 0$ or, equivalently, $\psi_x = \psi_y = 0$, at $x = 0$. The no normal flow boundary condition, $\psi_y = 0$, is equivalent to saying that $\psi$ is constant along the boundary. Since we can always add or subtract a constant from our definition of $\psi$ and get the same flow field, let's pick $\psi = 0$ as the constant at the boundary. This boundary condition can then be written in terms of $\widetilde{\psi}$

$$\widetilde{\psi}^{(1)}(x = 0) = -\psi^I(x = 0) = -G(y), \tag{6.38}$$

or

$$C(y)cos(D(y)) = -G(y). \tag{6.39}$$

The second boundary condition, $v(x = 0) = 0$ can be written

$$\frac{\partial}{\partial x}\widetilde{\psi}^{(1)} = \frac{\partial \widetilde{\psi}^{(1)}}{\partial \widetilde{x}}\frac{d\widetilde{x}}{dx} = \epsilon^{-1/3}\widetilde{\psi}^{(1)}_{\widetilde{x}} = -\psi^I_x, \quad @ \quad x = 0, \tag{6.40}$$

or

$$\epsilon^{-1/3}(-\frac{1}{2}\beta^{1/3})C(y)cos(D(y)) - \epsilon^{-1/3}\frac{\sqrt{3}}{2}\beta^{1/3}C(y)sin(D(y)) = -\frac{W}{\beta}. \tag{6.41}$$

Since we are looking in the limit when $\epsilon \to 0$, this is equivalent to

$$-\frac{1}{2}\beta^{1/3}C(y)cos(D(y)) = \frac{\sqrt{3}}{2}\beta^{1/3}C(y)sin(D(y)), \tag{6.42}$$

or

$$tan(D(y)) = -\frac{1}{\sqrt{3}}, \tag{6.43}$$

which implies

$$D = -\frac{\pi}{6}. \tag{6.44}$$

Plugging back into Eq. (6.39) gives

$$C(y) = \frac{-2}{\sqrt{3}}G(y). \tag{6.45}$$

Finally, we have our solution for the boundary layer correction in region (1):

$$\widetilde{\psi}^{(1)} = \frac{-2G(y)}{\sqrt{3}}e^{-\beta^{1/3}\widetilde{x}/2}cos\left(\frac{\sqrt{3}}{2}\beta^{1/3}\widetilde{x} - \frac{\pi}{6}\right). \tag{6.46}$$

Now, we need to find the boundary layer correction in region (2), the eastern boundary. Luckily, we have already done most of the work. The eastern boundary layer ends at $x = L$ where we need to apply construct $\widetilde{\psi}^{(2)}$ to meet the boundary conditions. Again, we will rescale our $x$ coordinate, but this time let $\widetilde{x} = 0$ correspond to the boundary:

$$\widetilde{x} = \frac{x - L}{\epsilon^a}. \tag{6.47}$$

For the same reason as before, we need $a = 1/3$. Here, the boundary layer correction obeys the same equation as in the western boundary, so our general solution, given in Eq. (6.36) is the same. In the eastern boundary coordinates, however, we require that

$$\widetilde{\psi}^{(2)} \to 0, \quad \text{as}, \quad \widetilde{x} \to -\infty. \tag{6.48}$$

This implies that $A(y) = C(y) = D(y) = 0$, and

$$\widetilde{\psi}^{(2)} = B(y)e^{\beta^{1/3}\widetilde{x}}. \tag{6.49}$$

Applying the no slip boundary condition, we have

$$\epsilon^{-1/3}\widetilde{\psi}^{(2)} = -\psi_x^I, \quad @ \quad x = L, \tag{6.50}$$

or

$$\epsilon^{-1/3}\beta^{1/3}B(y) = -\frac{W(y)}{\beta}, \tag{6.51}$$

implying that

$$B(y) = \frac{-\epsilon^{1/3}W(y)}{\beta^{4/3}}. \tag{6.52}$$

Our second boundary condition is that $\psi(x = L) = 0$. Notice, however, that $B(y) \to 0$ as $\epsilon \to 0$, so we can't use $\widetilde{\psi}$ to match this boundary condition. This means that the interior solution itself must meet this boundary condition. Fortunately, we haven't yet specified $G(y)$, so the no normal flow boundary condition $\psi(x = L) = 0$ requires that

$$G(y) = -\frac{W(y)L}{\beta}. \tag{6.53}$$

The solution to the boundary layer correction along the eastern boundary is then

$$\widetilde{\psi}^{(2)} = -\epsilon^{1/3}W(y)\beta^{-4/3}e^{\beta^{1/3}\widetilde{x}}. \tag{6.54}$$

Notice that unlike $\widetilde{\psi}^{(1)}$, which was $O(1)$, $\widetilde{\psi}^{(2)}$ is $O(\epsilon^{1/3})$. This implies that the boundary layer correction on the eastern boundary is much smaller than the correction on the western boundary. As we will see, this means that the gradients in $\psi$ are much larger on the western side, and this is why the western boundary currents like the Gulf Stream are much stronger than those on the eastern side of the basins.

Combining the solutions for the boundary layer corrections in Eq. (6.46) and (6.54) into Eq. (6.21) gives our full solution. Using $\widetilde{x} = x\epsilon^{-1/3}$ in $\widetilde{\psi}^{(1)}$, $\widetilde{x} = (x - L)\epsilon^{-1/3}$ in $\widetilde{\psi}^{(2)}$ and $\epsilon = \nu$, we can write the solution that is valid for all $x$:

$$\psi = \frac{x - L}{\beta}W(y) + \frac{2W(y)L}{\sqrt{3}\beta}e^{-\beta^{1/3}x/(2\nu^{1/3})}cos\left(\frac{\sqrt{3}}{2}\beta^{1/3}\nu^{-1/3}x - \frac{\pi}{6}\right) - \nu^{1/3}\beta^{-4/3}W(y)e^{\beta^{1/3}\nu^{-1/3}(x-L)}. \tag{6.55}$$

So far we haven't dealt with the boundaries at the top and bottom of our rectangular basin. We could go through a similar procedure to obtain a solution that satisfies these boundary conditions. However, notice that $W(y)$ multiplies every term in $\psi$. Since the north/south boundary conditions are that $\psi = 0$ and $\psi_x = 0$, we automatically meet both of these boundary conditions as long as $W = 0$ at the boundaries.

Figure 15 shows the solution in Eq. (6.55) with a parabolic wind stress curl, $W(y) = (y - \frac{1}{2})^2 - \frac{1}{4}$ which was chosen to vanish at the upper and lower boundaries (in this case $y = 0$ and $y = 1$). Like the region between the trade winds and the westerlies in the northern hemisphere, $W(y)$ is negative inside our domain. Since the velocity is $v = \psi_x$ and $u = -\psi_y$, we see that there is a strong northward flow inside the western boundary layer, and a much weaker return flow throughout the rest of the basin. Essentially, our gyre circulation has shifted to give a very strong western boundary current.

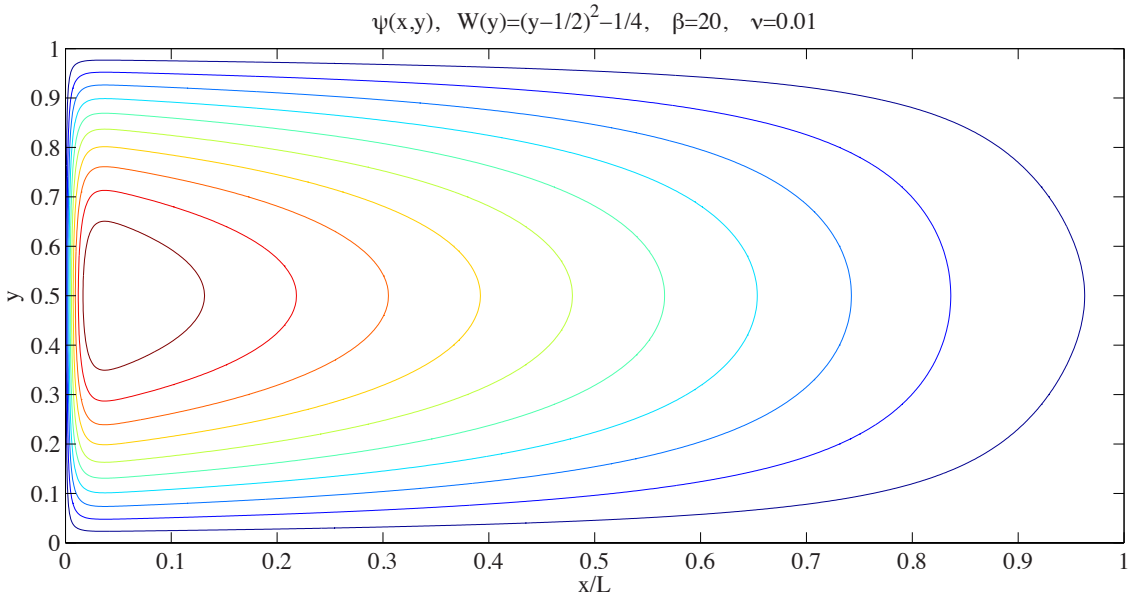


Figure 15: The full solution for $\psi$ with a negative, parabolic wind stress curl.

# 7 Vertical velocity, frontogenesis, and the Omega equation

So far, in looking at large scale processes in the ocean and atmosphere, we have focussed mostly on horizontal motions. Although generally much smaller than their horizontal counterparts, vertical motion is also very important. In the atmosphere, rising air drives cloud formation and precipitation. In the ocean, upwelling water supplies nutrients to phytoplankton which form the base of the marine food web. We can say a remarkable amount about the vertical velocity from the QG equations that we have already seen in detail. This analysis will also allow us to examine the formation of fronts, or *frontogenesis*, and will show that the QG equations predict their own demise!

Let's start with the equations for a stratified, inviscid, boussinesq fluid on an $f$-plane:

$$\frac{D\mathbf{u}_H}{Dt} + f\hat{k} \times \mathbf{u} = -\nabla p, \tag{7.1}$$

$$0 = -\frac{\partial p}{\partial z} + b, \tag{7.2}$$

$$\nabla \cdot \mathbf{u} = 0, \tag{7.3}$$

$$\frac{Db}{Dt} + wN^2 = 0. \tag{7.4}$$

In the last equation for buoyancy, we have decomposed the total buoyancy into perturbations about the background stratification, i.e. $b_T = b(x, y, z, t) + N^2 z$ where $b_T$ is the full buoyancy. Now, decompose the horizontal velocity into *geostrophic* and*ageostrophic* components

$$\mathbf{u}_H = \mathbf{u}_g + \mathbf{u}_{ag}, \tag{7.5}$$

where, by definition, the geostrophic part satisfies

$$f\hat{k} \times \mathbf{u}_g = -\nabla_H p. \tag{7.6}$$

Notice from Eq. (7.6) that $-p/f$ acts like a streamfunction for the geostrophic flow since $\mathbf{u}_g = -\nabla_H \times p/f$, where $\mathbf{f} = f\hat{k}$ since we are considering an $f$-plane. We also see from this equation that the geostrophic flow will always be non-divergent, $\nabla \cdot \mathbf{u}_g = 0$. The continuity equation then becomes

$$\nabla_H \cdot \mathbf{u}_{ag} + \frac{\partial w}{\partial z} = 0, \tag{7.7}$$

and we see that the vertical velocity, $w$, is the same order as the *ageostrophic* velocity. One of the QG assumptions is that the Rossby number is small, or that the flow is dominated by the geostrophic velocity

$$\mathbf{u}_{ag} << \mathbf{u}_g. \tag{7.8}$$

Using Eq. (7.6) in Eqns. (7.4) and neglecting $\mathbf{u}_{ag}$ compared to $\mathbf{u}_g$ gives

$$\left(\frac{\partial}{\partial t} + \mathbf{u}_g \cdot \nabla_H\right) \mathbf{u}_g + f\hat{k} \times \mathbf{u}_{ag} = 0, \tag{7.9}$$

$$\nabla_H \cdot \mathbf{u}_{ag} + \frac{\partial w}{\partial z} = 0, \tag{7.10}$$

$$\left(\frac{\partial}{\partial t} + \mathbf{u}_g \cdot \nabla_H\right) b + wN^2 = 0. \tag{7.11}$$

Now, let's take the $z$-derivative of the $x$-momentum equation:

$$\left(\frac{\partial}{\partial t} + \mathbf{u}_g \cdot \nabla_H\right) \frac{\partial u_g}{\partial z} + \frac{\partial \mathbf{u}_g}{\partial z} \cdot \nabla_H u_g - f\frac{\partial v_{ag}}{\partial z} = 0, \tag{7.12}$$

and the $y$-derivative of the buoyancy equation:

$$\left(\frac{\partial}{\partial t} + \mathbf{u}_g \cdot \nabla_H\right)\frac{\partial b}{\partial y} + \frac{\partial \mathbf{u}_g}{\partial y} \cdot \nabla_H b + N^2 \frac{\partial w}{\partial y} = 0. \tag{7.13}$$

Recall from the thermal wind relation that

$$f\frac{\partial u_g}{\partial z} = -\frac{\partial b}{\partial y}. \tag{7.14}$$

Multiplying by $f$, Eq. (7.12) then becomes

$$-\left(\frac{\partial}{\partial t} + \mathbf{u}_g \cdot \nabla_H\right)\frac{\partial b}{\partial y} + f\frac{\partial \mathbf{u}_g}{\partial z} \cdot \nabla_H u_g - f^2\frac{\partial v_{ag}}{\partial z} = 0. \tag{7.15}$$

Adding Eq. (7.13) and (7.15) eliminates the material time derivative:

$$\frac{\partial \mathbf{u}_g}{\partial y} \cdot \nabla_H b + N^2\frac{\partial w}{\partial y} + f\frac{\partial \mathbf{u}_g}{\partial z} \cdot \nabla_H u_g - f^2\frac{\partial v_{ag}}{\partial z} = 0, \tag{7.16}$$

or, writing out each term:

$$\frac{\partial u_g}{\partial y}\frac{\partial b}{\partial x} + \frac{\partial v_g}{\partial y}\frac{\partial b}{\partial y} - \frac{\partial u_g}{\partial x}\frac{\partial b}{\partial y} + \frac{\partial u_g}{\partial y}\frac{\partial b}{\partial x} + N^2\frac{\partial w}{\partial y} - f^2\frac{\partial v_{ag}}{\partial z} = 0. \tag{7.17}$$

However, since $\partial v_g/\partial y = -\partial u_g/\partial x$ from the continuity equation, we can re-write Eq. (7.17) as

$$N^2\frac{\partial w}{\partial y} - f^2\frac{\partial v_{ag}}{\partial z} = -2\frac{\partial u_g}{\partial y}\frac{\partial b}{\partial x} + 2\frac{\partial u_g}{\partial x}\frac{\partial b}{\partial y}. \tag{7.18}$$

Working through a similar analysis, starting with the $y$-momentum equation, gives us a second equation

$$N^2\frac{\partial w}{\partial x} - f^2\frac{\partial u_{ag}}{\partial z} = -2\frac{\partial v_g}{\partial y}\frac{\partial b}{\partial x} + 2\frac{\partial v_g}{\partial x}\frac{\partial b}{\partial y}. \tag{7.19}$$

Finally, taking $\partial/\partial_y$ of Eq. (7.18) and $\partial/\partial_x$ of Eq. (7.19), adding the results, and using $\partial u_{ag}/\partial x + \partial v_{ag}/\partial y = -\partial w/\partial z$ gives

$$N^2\nabla_H^2 w + f^2\frac{\partial^2 w}{\partial z^2} = 2\nabla_H \cdot \mathbf{Q} \tag{7.20}$$

where

$$\mathbf{Q} = \left(-\frac{\partial v_g}{\partial y}\frac{\partial b}{\partial x} + \frac{\partial v_g}{\partial x}\frac{\partial b}{\partial y}, -\frac{\partial u_g}{\partial y}\frac{\partial b}{\partial x} + \frac{\partial u_g}{\partial x}\frac{\partial b}{\partial y}, 0\right). \tag{7.21}$$

Equation (7.20) is known as the *omega equation* because the symbol $\omega$ is often used to denote vertical velocity in atmospheric science. The vector $\mathbf{Q}$ is known simply as the *Q-vector*. The omega equation gives us a diagnostic tool to predict the vertical velocity given the three-dimensional pressure and buoyancy (or temperature) fields. This analysis is often used in meteorology, and you can sometimes find maps of $\mathbf{Q}$ and its divergence in atmospheric model forecasts.

Although we could solve Eq. (7.20) numerically, we can get a qualitative sense for the vertical velocity much more easily. Suppose that the vertical velocity takes the form of a plane wave in $x$ and $y$, and is described by the lowest mode in the vertical

$$w = \hat{w}e^{ikx+ily}sin\left(\frac{\pi z}{H}\right), \tag{7.22}$$

so that $w = 0$ at $z = 0$ (the ground or the seafloor) and at $z = H$ (the troposphere or the top of the ocean). Using this form in the omega equation gives

$$w = \frac{-2\nabla \cdot \mathbf{Q}}{N^2|\mathbf{k}|^2 + f^2\pi^2/H^2}. \tag{7.23}$$

From this equation, we see that $w$ will tend to vary inversely with the divergence of $Q$:

$$\nabla \cdot \mathbf{Q} < 0 \quad \rightarrow \quad w > 0, \tag{7.24}$$
$$\nabla \cdot \mathbf{Q} > 0 \quad \rightarrow \quad w < 0. \tag{7.25}$$

Although this relation isn't exact, it gives us a very useful rule of thumb.

In addition to predicting the vertical velocity, the Q-vector also gives us information about where fronts, or regions with large density gradients, are likely to form. Fronts are clearly important in the atmosphere and are associated with some of our most violent weather. In the ocean, recent studies are finding that fronts are hotspots for biological productivity.

Let's start by considering the buoyancy equation from before, along a boundary, where $w = 0$:

$$\frac{\partial b}{\partial t} + \mathbf{u}_g \cdot \nabla b = 0. \tag{7.26}$$

Taking $\partial_x$ and $\partial_y$ of Eq. (7.26) gives

$$(\partial_t + \mathbf{u} \cdot \nabla_H)\frac{\partial b}{\partial x} + \frac{\partial \mathbf{u}_g}{\partial x} \cdot \nabla b = 0, \tag{7.27}$$
$$(\partial_t + \mathbf{u} \cdot \nabla_H)\frac{\partial b}{\partial y} + \frac{\partial \mathbf{u}_g}{\partial y} \cdot \nabla b = 0, \tag{7.28}$$

or

$$\frac{D_g}{Dt}\left(\frac{\partial b}{\partial x}\right) = -\frac{\partial u_g}{\partial x}\frac{\partial b}{\partial x} - \frac{\partial v_g}{\partial x}\frac{\partial b}{\partial y}, \tag{7.29}$$
$$\frac{D_g}{Dt}\left(\frac{\partial b}{\partial y}\right) = -\frac{\partial u_g}{\partial y}\frac{\partial b}{\partial x} - \frac{\partial v_g}{\partial y}\frac{\partial b}{\partial y}. \tag{7.30}$$

Where $D_g/Dt$ is a material derivative moving with the geostrophic flow. Using $\partial u_g/\partial x = -\partial v_g/\partial y$ in the first equation, and $\partial v_g/\partial y = -\partial u_g/\partial x$ in the second equation, we see that

$$\frac{D_g}{Dt}\nabla_H b = \mathbf{Q}, \tag{7.31}$$

where $\mathbf{Q}$ is the Q-vector defined in Eq. 7.21. Taking the dot product of $\nabla_H b$ with the above equation gives

$$\frac{D_g}{Dt}|\nabla_H b|^2 = 2\mathbf{Q} \cdot \nabla_H b. \tag{7.32}$$

This equation gives us the rate of change of the frontal strength in a coordinate frame moving with the geostrophic flow. The left hand side of Eq. (7.32) is called the *frontogenesis function*, and controls whether a front will strengthen or weaken.

## References